

General Disclaimer

One or more of the Following Statements may affect this Document

- This document has been reproduced from the best copy furnished by the organizational source. It is being released in the interest of making available as much information as possible.
- This document may contain data, which exceeds the sheet parameters. It was furnished in this condition by the organizational source and is the best copy available.
- This document may contain tone-on-tone or color graphs, charts and/or pictures, which have been reproduced in black and white.
- This document is paginated as submitted by the original source.
- Portions of this document are not fully legible due to the historical nature of some of the material. However, it is the best reproduction available from the original submission.

JPL PUBLICATION 84-94, REVISION 1

(NASA-CR-175878) PERFORMANCE ANALYSIS OF
THE DSN BASEBAND ASSEMBLY (BBA) REAL-TIME
COMBINER (RTC) (Jet Propulsion Lab.) 53 p
HC A04/MF A01 CSCL 17B

N85-28190

G3/32 Unclas
21431

Performance Analysis of the DSN Baseband Assembly (BBA) Real-Time Combiner (RTC)

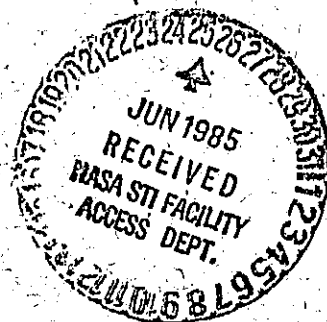
Marvin K. Simon
Alex Milleant

May 1, 1985

NASA

National Aeronautics and
Space Administration

Jet Propulsion Laboratory
California Institute of Technology
Pasadena, California



JPL PUBLICATION 84-94, REVISION 1

Performance Analysis of the DSN Baseband Assembly (BBA) Real-Time Combiner (RTC)

Marvin K. Simon
Alex Mileant

May 1, 1985



National Aeronautics and
Space Administration

Jet Propulsion Laboratory
California Institute of Technology
Pasadena, California

The research described in this publication was carried out by the Jet Propulsion Laboratory, California Institute of Technology, under a contract with the National Aeronautics and Space Administration.

Reference herein to any specific commercial product, process, or service by trade name, trademark, manufacturer, or otherwise, does not constitute or imply its endorsement by the United States Government or the Jet Propulsion Laboratory, California Institute of Technology.

ABSTRACT

The operation of the BBA Real-Time Combiner (RTC) is discussed and its performance investigated in detail. It is shown that each channel of the RTC can be modelled by a simple block diagram in the z-transform domain from which all pertinent transient and steady state behavioral characteristics can be determined. In particular, the characteristic equation of the tracking loop and its equivalent noise bandwidth are found and used to evaluate the closed loop transient response and steady-state mean squared timing jitter. The impact of the totality of these loop jitter contributions on the combiner output SNR is evaluated and illustrated numerically. These results show that for parameters of interest to various space missions, the RTC is capable of providing significant SNR improvement relative to a single receiving antenna.

PREFACE TO REVISION 1

This report has been revised to correct a computational error in certain results that was found after publication. The corrected performance calculations have been made and included in this revision. The figures affected by this revision are Figures 12 through 17. Figure 3 has also been corrected.

CONTENTS

I.	INTRODUCTION	1
II.	STATISTICS OF THE ERROR SIGNAL	6
	A. ERROR SIGNAL STATISTICS FOR RANDOM DATA	10
	B. ERROR SIGNAL STATISTICS FOR DATA PLUS SUBCARRIER	14
III.	RTC LAPLACE TRANSFORM BLOCK DIAGRAM AND TRANSFER FUNCTION	18
IV.	NOISE ANALYSIS	25
V.	DELAY RATE COMPENSATION	28
VI.	OPTIMUM COHERENT COMBINING	30
VII.	DEGRADATION OF THE SUMMER OUTPUT SIGNAL-TO-NOISE RATIO (SNR) DUE TO DELAY JITTER	33

Figures

1.	Multiple Antenna Arraying System	2
2.	Baseband Assembly	3
3.	Real-Time Combiner	5
4.	RTC Cross-Correlator	7
5.	Timing Diagram	11
6.	Delay Error Versus Time	13
7.	Contributors to XOR Gate Output as a Function of Delay:	
	(a) Deterministic, Same Polarity	15
	(b) Deterministic, Opposite Polarity	15
	(c) Contribution of Symbol Transition, Opposite Polarity	15
	(d) Contribution of Symbol Transition, Same Polarity	15
8.	RTC Laplace Transform Block Diagram	20

CONTENTS (Continued)

9.	RTC Equivalent Block Diagram in z Domain	21
10.	Root Locus Diagram	23
11.	BBA Signal Combiner Model	31
12.	Degradation Factor vs. Symbol SNR, Voyager Mission, L = 2	40
13.	Degradation Factor vs. Symbol SNR, Voyager Mission, L = 4	41
14.	Degradation Factor vs. Symbol SNR, Pioneer Mission, L = 2	42
15.	Degradation Factor vs. Symbol SNR, Pioneer Mission, L = 4	43
16.	Degradation Factor vs. Symbol SNR, VRM Mission, L = 2	44
17.	Degradation Factor vs. Symbol SNR, VRM Mission, L = 4	45

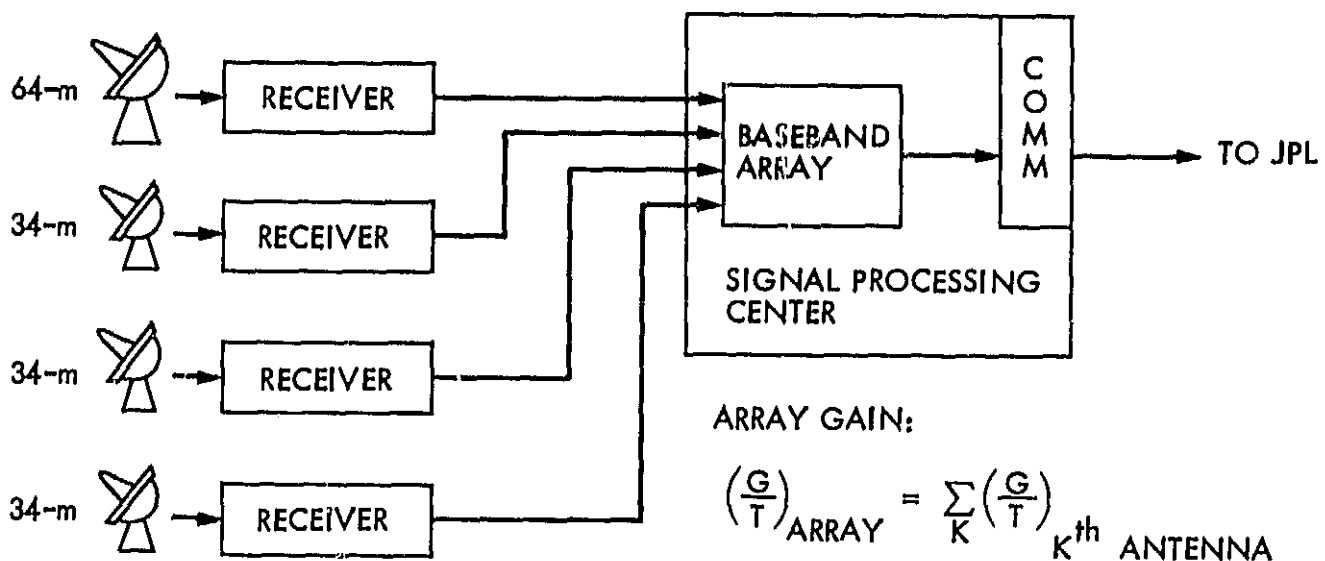
Table

1.	Noise Equivalent Bandwidth in Hz vs. Loop Gain AG and Computation Time Factor g	26
----	--	----

SECTION I
INTRODUCTION

The Deep Space Network (DSN) is responsible for providing interplanetary communications for the National Aeronautics and Space Administration (NASA). A key feature of the DSN system is the improvement in effective antenna aperture gained by combining the outputs of a number of antennas in the network, i.e., multiple antenna arraying (see Figure 1). In particular, if system performance is measured in terms of the ratio of system gain to system noise temperature (G/T), then the effective G/T after arraying is theoretically equal to the sum of the G/T 's corresponding to the individual antennas being combined. More realistically, one must have available a detailed analysis of the array combining system accounting for all real losses in order to identify how much of the above theoretical limit is practically achievable after signal processing. The purpose of this report is to provide such an analysis from which estimates of performance degradation from the ideal case can be assessed in terms of actual system design parameters. The final analytical results will be numerically illustrated with several examples corresponding to actual deep space mission designs.

Figure 2 shows the basic structure of the Baseband Assembly (BBA). Its purpose is to combine coherently signals from several antennas and perform sub-carrier demodulation and symbol synchronization on the combined signal. The BBA consists of three main devices: the Real-Time Combiner (RTC), the Sub-carrier Demodulation Assembly (SDA) and the Symbol Synchronization Assembly (SSA). The last two assemblies are often designated as a single assembly, the Demodulation Synchronization Assembly (DSA). The inputs to the BBA are analog



TYPICAL DSN COMPLEX
(AUSTRALIA, CALIFORNIA, SPAIN)

Figure 1. Multiple Antenna Arraying System

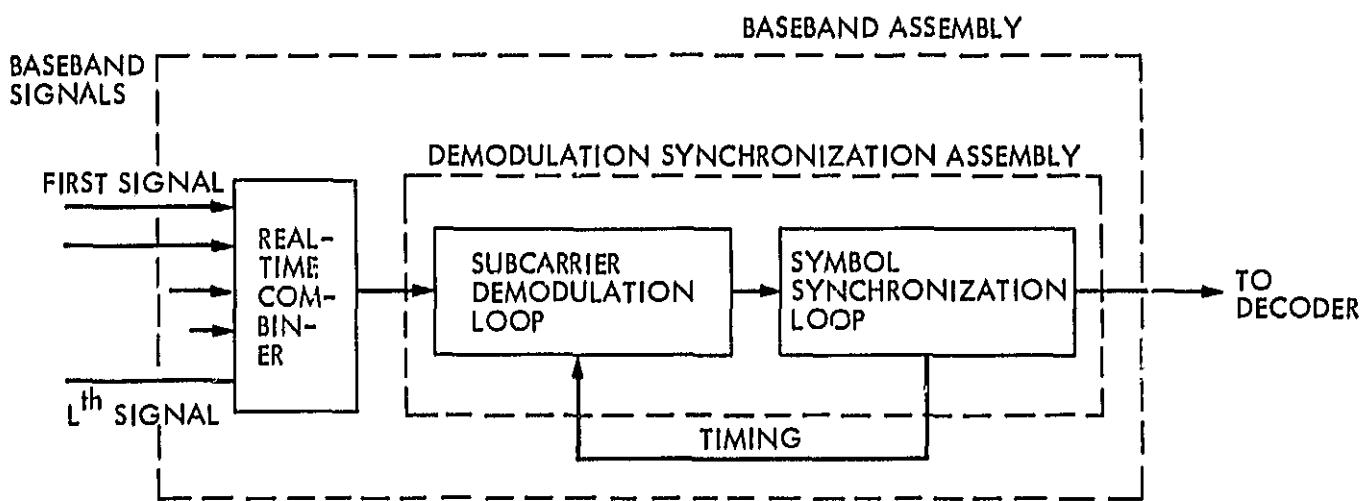


Figure 2. Baseband Assembly

baseband telemetry signals from L receivers. These signals are low-pass filtered, sampled, and digitized. After that, all the processes performed in the BBA pertaining to time alignment, subcarrier demodulation and symbol synchronization may be looked upon as purely digital operations on unitless numbers.

In this report, the operation of the RTC will be discussed. The purpose of the RTC is to time-align signals from different antennas in order to increase the strength of the total combined signal. The basic structure of the RTC is illustrated in Figure 3. After low-pass filtering and analog-to-digital (A/D) conversion, the signals from $L-1$ different antennas are cross-correlated with the master or reference signal. These cross-correlations produce error signals proportional to the relative time delays between these and the reference antenna. The error signals are read by the CPU every T_L seconds (duration of K data symbols), which produces time delays in the First-In-First-Out (FIFO) devices in order to compensate for the misalignments. Finally, the signals are multiplied by weighting factors and summed in the combiner. The combined signal goes to the DSA for further processing.

The analysis of the RTC's performance will be subdivided into the following categories:

1. Statistics of the Error Signal
2. RTC Laplace Transform Block Diagram and Transfer Function
3. Noise Analysis
4. Delay Rate Compensation
5. Optimum Coherent Combining
6. Degradation of the Summer Output Signal-to-Noise Ratio (SNR) Due to Delay Jitter

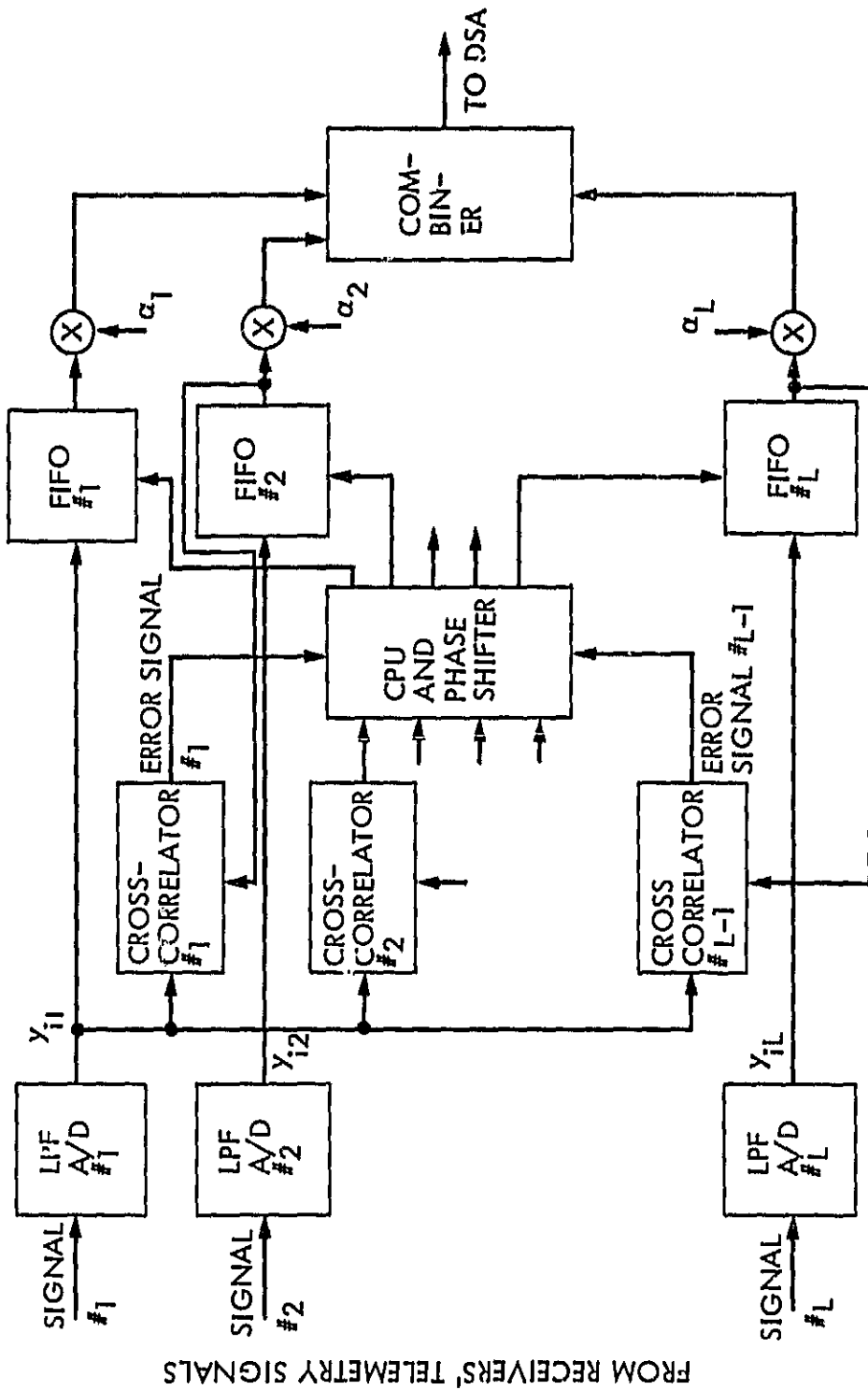


Figure 3. Real-Time Combiner

SECTION II

STATISTICS OF THE ERROR SIGNAL

Baseband signals from L antennas are sampled at the Nyquist rate r_N samples/sec. Each sample is converted to an 8-bit binary word by an A/D converter. The most significant bit of each sample represents the sign of its voltage: a "0" corresponds to a positive voltage and a "1" corresponds to a negative voltage. The A/D output corresponding to the first antenna (herein referred to as the master or reference antenna) is cross-correlated with the outputs of each of the other $L-1$ A/D's to form a set of error signals proportional to the difference in time delay between the reference and the j^{th} antenna, $j = 2, 3, \dots, L$.

The basic structure of the $L-1$ identical quadrature correlators is shown in Figure 4. Let y_{ij} represent the i^{th} sample of the j^{th} antenna A/D output and, in particular, y_{i1} represents the i^{th} sample of the reference antenna A/D output. Then, in the upper arm of the j^{th} correlator, the sign bit of y_{ij} is exclusive ORed (XOR) with a delayed (N_d samples) version of the sign bit of y_{i1} , while in the lower arm, the sign bit of y_{i1} is XORed with a delayed version of the sign bit of y_{ij} . The truth table for the XOR operation with arbitrary inputs A and B is given below:

<u>A</u>	<u>B</u>	<u>XOR</u>
0	0	0
0	1	1
1	0	1
1	1	0

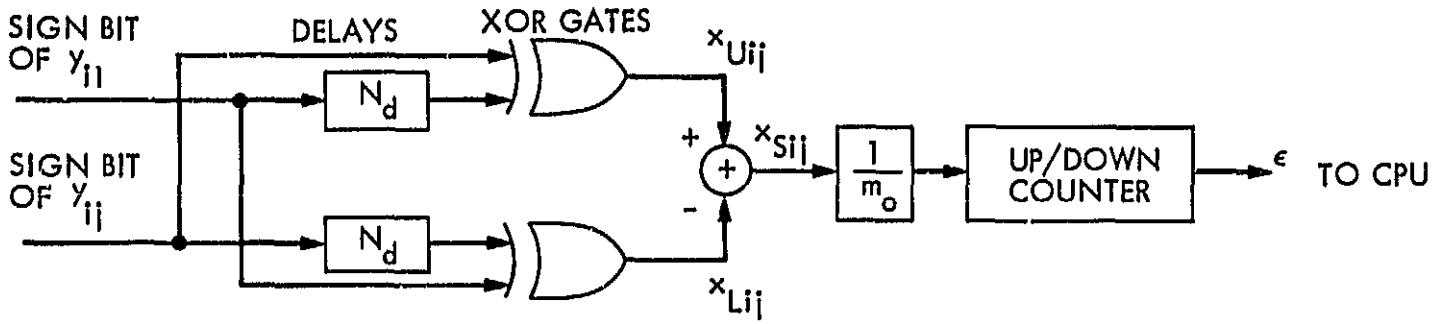


Figure 4. RTC Cross-Correlator

At the output of the XOR gates, the signals x_{i1} and x_{ij} assume values "0" and "1" according to the above table. The sample x_{Lij} is subtracted from x_{Uij} to produce x_{Sij} , which, after prescaling, goes to a counter. The output of the counter is called the error signal and is a random variable whose mean and variance are vital to a determination of the RTC's performance. In the ensuing analysis, we shall derive these two moments.

The i^{th} sample of the j^{th} signal, y_{ij} , is modelled as the random variable

$$y_{ij} = s_{ij} + n_{ij} \quad (1)$$

where s_{ij} and n_{ij} , respectively, represent the signal and noise components of the input signal. The first and second moments of y_{ij} are given by and

$$\begin{aligned} E\{y_{ij}\} &= \sqrt{S_j} \\ E\{y_{ij}^2\} &= E\{n_{ij}^2\} + S_j = \sigma_{nj}^2 + S_j \end{aligned} \quad (2)$$

where $\sqrt{S_j}$ represents the amplitude of the j^{th} signal and σ_{nj} is the rms noise amplitude in the j^{th} channel. Thus,

$$\sigma_{nj}^2 = N_{0j} B_{nj} \quad (3)$$

where N_{0j} is the one-sided noise spectral density and B_{nj} is the one-sided baseband bandwidth at the BBA j^{th} input.

If the signals coming from the reference and the j^{th} antenna were noise-free and perfectly aligned, then the output of the correlator, x_{Sij} , would be zero all of the time. However, noise introduces randomness into the values of y_{i1} and y_{ij} . The probability that y_{i1} will flip from "0" to "1" or vice versa is

$$p_1 = \frac{1}{2} \operatorname{erfc} \left(\sqrt{\frac{s_1}{2\sigma_{n1}^2}} \right) \quad (4)$$

and the probability that y_j will do the same is

$$p_j = \frac{1}{2} \operatorname{erfc} \left(\sqrt{\frac{s_j}{2\sigma_{nj}^2}} \right) \quad (5)$$

where $\operatorname{erfc} x \triangleq 1 - \operatorname{erf} x$ is the complementary error function defined by

$$\operatorname{erfc} x = \frac{2}{\sqrt{\pi}} \int_x^\infty \exp(-y^2) dy \quad (6)$$

Then, in terms of p_1 and p_j , the probability that x_{Uij} or x_{Lij} will be in error is

$$\begin{aligned} p_{ej} &= (1-p_1)p_j + (1-p_j)p_1 \\ &= \frac{1}{2} \left[1 - \operatorname{erf} \left(\sqrt{\frac{s_1}{2\sigma_{n1}^2}} \right) \operatorname{erf} \left(\sqrt{\frac{s_j}{2\sigma_{nj}^2}} \right) \right] \end{aligned} \quad (7)$$

or, alternately, the probability that x_{Uij} or x_{Lij} is correct is

$$p_{cj} = 1 - p_{ej} = \frac{1}{2} \left[1 + \operatorname{erf} \left(\sqrt{\frac{s_1}{2\sigma_{n1}^2}} \right) \operatorname{erf} \left(\sqrt{\frac{s_j}{2\sigma_{nj}^2}} \right) \right] \quad (8)$$

Given that y_1 and y_j are both equally likely to be a "0" or "1", then the expected value of x_{Uij} or x_{Lij} is

$$E\{x_{\alpha ij}\} = 0 \times (1-p_{ej}) + 1 \times p_{ej} = p_{ej}; \quad \alpha = U \text{ or } L \quad (9)$$

Define s_j as follows:

$$s_j = \sum_{i=1}^N x_{\alpha ij} \quad (10)$$

Then, since random variables $x_{\alpha ij}$; $\alpha = U$ or L , $j = 1, 2, \dots, L$ correspond to Nyquist samples, they are independent (with respect to the index i) and have first and second moments

$$E\{s_j\} = Np_{ej} \quad (11)$$

$$E\{s_j^2\} = Np_{ej} + N(N-1)p_{ej}^2 \quad (12)$$

and variance

$$\sigma_j^2 = E\{s_j^2\} - (E\{s_j\})^2 = Np_{ej}(1-p_{ej}) \quad (13)$$

Substituting Eq. (7) into Eq. (13) gives

$$\sigma_j^2 = \frac{N}{4} \left\{ 1 - \left[\operatorname{erf} \left(\sqrt{\frac{s_1}{2\sigma_{n1}^2}} \right) \operatorname{erf} \left(\sqrt{\frac{s_j}{2\sigma_{nj}^2}} \right) \right]^2 \right\} \quad (14)$$

When the above steps are repeated with y_{i1} and y_{ij} having opposite signs, the same variance is obtained. Hence, the variance is independent of the transitions of the signal and is the same for deterministic and random data.

After this preliminary discussion, the means and variances of the error signal will be derived for two classes of data:

1. Random data
2. Random data plus subcarrier

A. ERROR SIGNAL STATISTICS FOR RANDOM DATA

Let N_s be the number of Nyquist samples per symbol and p_T be the probability of symbol transition. Because of the delays in the arrival of the signal to different antennas and the delays in the correlator, the four streams of samples entering the two XOR gates of Figure 4 will have relative displacements as shown in Figure 5.

Referring to Figure 5, the expected number of "1"s, in the upper arm aver-

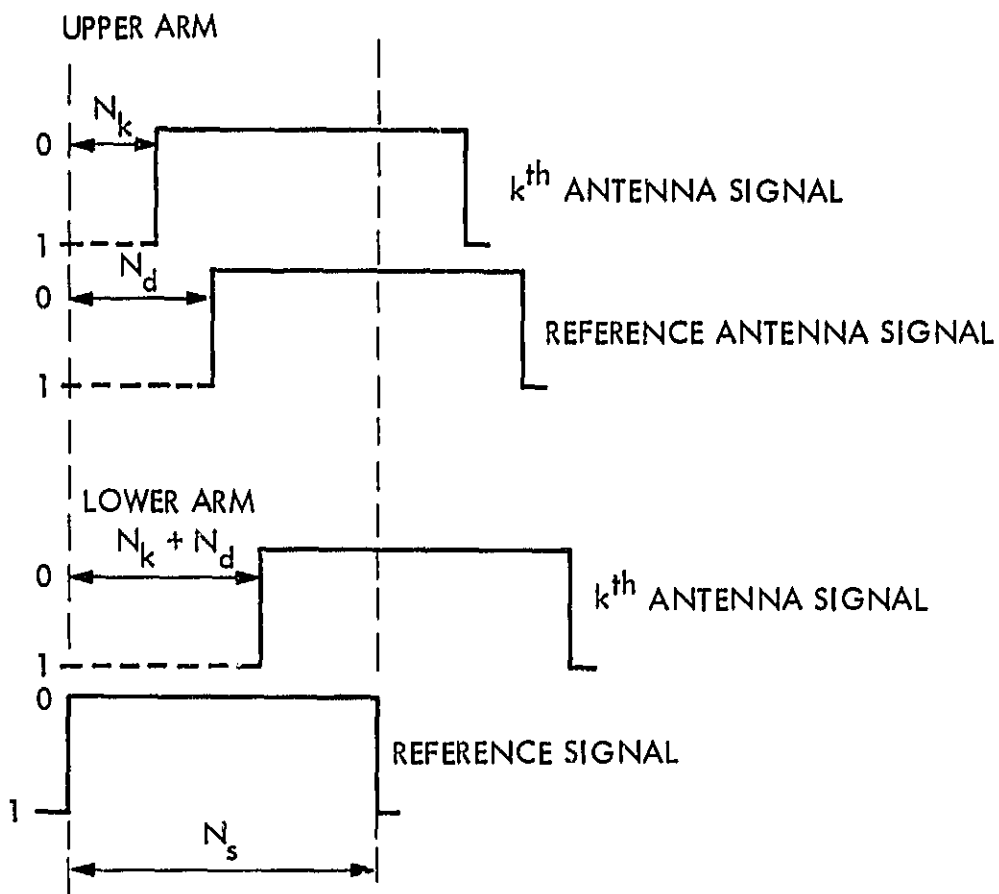


Figure 5. Timing Diagram

aged over one symbol time, will be*

$$\bar{x}_U = (N_S - N_U)p_e + (1-p_T)N_U p_e + p_T N_U (1-p_e) \quad (15)$$

where $N_U \triangleq N_d - N_k$ = the relative delay in the upper arm. Similarly, in the lower arm the expected number of "1"s will be

$$\bar{x}_L = (N_S - N_L)p_e + (1-p_T)N_L p_e + p_T N_L (1-p_e) \quad (16)$$

where $N_L \triangleq N_d + N_k$ = the relative delay in the lower arm. Subtracting \bar{x}_L from \bar{x}_U , we obtain the error signal, averaged over one symbol, namely,

$$\bar{x}_S = 2N_k p_T (2p_e - 1) \quad (17)$$

Here N_k is the relative delay of the two signals during the k^{th} symbol.

Since the number of symbols, K , in an update interval of T_L seconds is very large, we can model the delay error N_k at the instant k , by a continuous variable $N(t)$ (see Figure 6), in which case the average delay error over one update interval becomes

$$\bar{N}_e = \frac{1}{T_L} \int_{t-T_c}^{t+T_R} N(t) dt \quad (18)$$

where $T_L = T_c + T_R$. Here T_c denotes the computation time, i.e., the time required by the CPU to process the error signal sample, and T_R denotes the remainder of the update time interval.

The expected value of the error signal at the end of one (e.g., the n^{th}) update interval will be

*For simplicity of notation, we shall herein drop the subscripts i and j previously used to denote the particular sample and channel of interest, respectively. Whenever this is unclear, we shall reintroduce these dependencies.

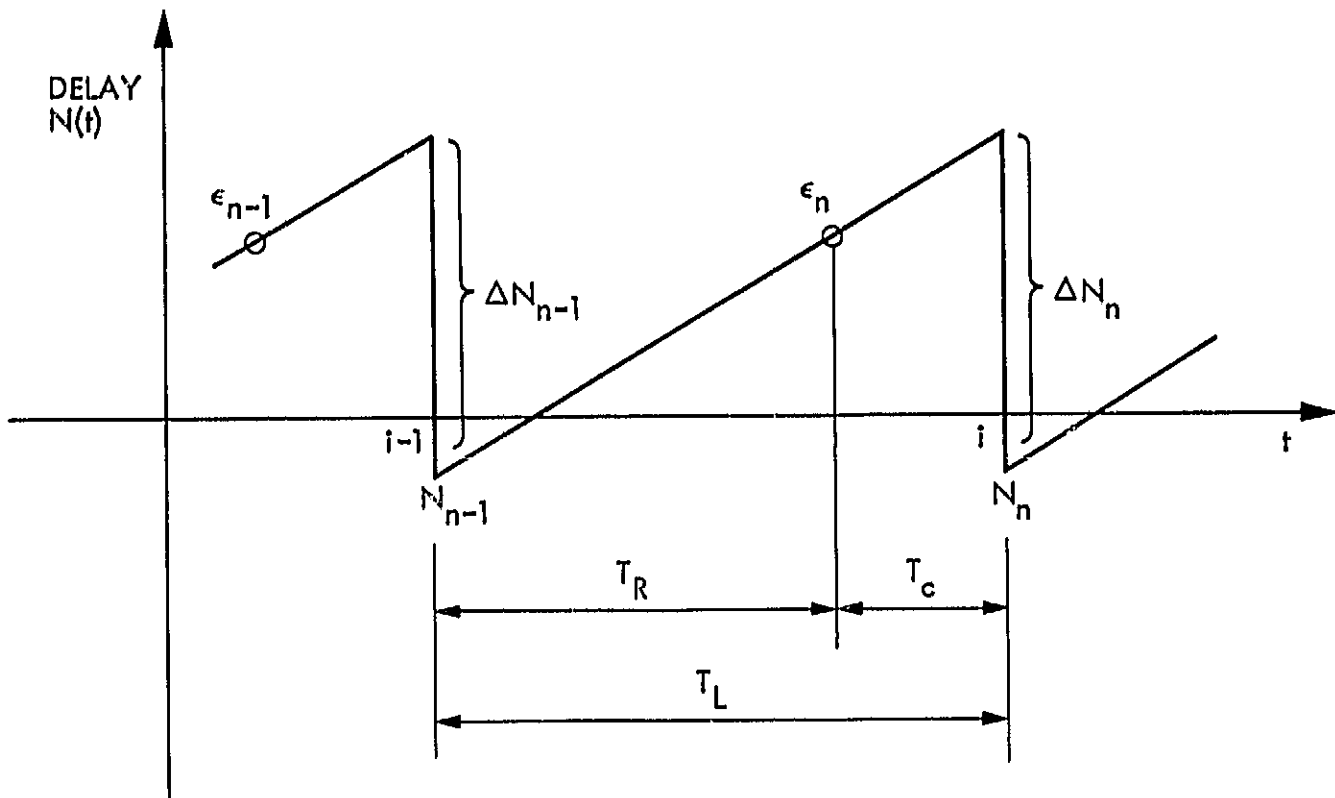


Figure 6. Delay Error Versus Time

$$\bar{\epsilon}_n = \frac{2K}{m_0} p_T (2p_e - 1) \bar{N}_e \quad (19)$$

where $1/m_0$ is the scaling factor at the input to the up/down counter (see Figure 4). Note that $\bar{\epsilon}_n = 0$ when $p_T = 0$, i.e., when no symbol transitions occur.

H. ERROR SIGNAL STATISTICS FOR DATA PLUS SUBCARRIER

Referring to Figure 7, when random data modulates a subcarrier of N_{sc} Nyquist samples per subcarrier period, then, in the upper arm, the expected number of "1"s averaged over one symbol period will be

$$\begin{aligned} \bar{x}_U = N_s (1 - 2N_U/N_{sc}) p_e + N_U (2N_s/N_{sc} - 1) (1 - p_e) \\ + p_T N_U p_e + (1 - p_T) (1 - p_e) N_U \quad \text{for } |N_U| \leq N_{sc}/2 \end{aligned} \quad (20)$$

A similar equation is obtained for the output of the lower arm, \bar{x}_L , with N_L substituted for N_U .

Subtracting again \bar{x}_L from \bar{x}_U we get

$$\bar{x}_S = N_k (2p_e - 1) f'_p \quad (21)$$

where

$$f'_p \triangleq 2 \left(\frac{2N_s}{N_{sc}} - p_T \right) \quad (22)$$

Note, that for large values of N_s/N_{sc} (the data period is much larger than the subcarrier period), the error signal is insensitive to the probability of symbol transition. This is true in the region $|N_k| \leq N_{sc}/2$ only. The error signal at the end of one update interval will be

$$\bar{\epsilon}_n = K \bar{N}_e (2p_e - 1) f'_p / m_0 \quad (23)$$

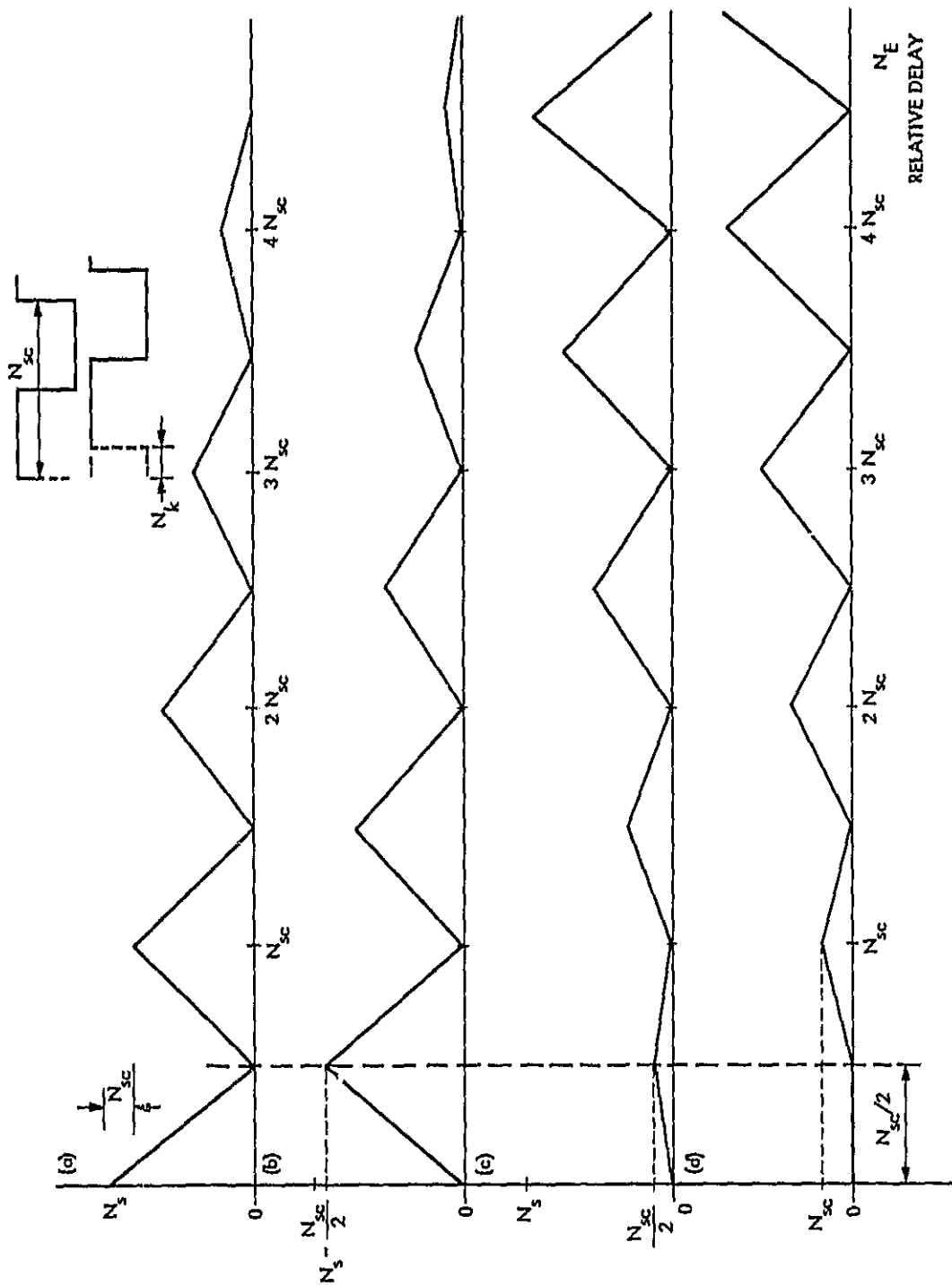


Figure 7. Contributors to XOR Gate Output as a Function of Delay: (a) Deterministic, Same Polarity, (b) Deterministic, Opposite Polarity, (c) Contribution of Symbol Transition, Opposite Polarity, and (d) Contribution of Symbol Transition, Same Polarity. The part in (a) is multiplied by p_e , and in (b) by $(1 - p_e)$; the parts in (c) and (d) depend on P_T .

Comparing Eq. (19) with Eq. (23), we can express the expected value of the error signal at the end of one update interval for both the random data and random data with subcarrier cases as

$$\bar{\epsilon}_n = G'_Q \bar{N}_e \quad (24)$$

where G'_Q is the gain which relates the average error signal at the end of an update interval to the average delay error over that interval and is defined by

$$\begin{aligned} G'_Q &\triangleq \frac{K}{m_o} (2p_e - 1) f_p \\ &= -\frac{K}{m_o} \operatorname{erf} \left(\sqrt{\frac{S_1}{2\sigma_{n1}^2}} \right) \operatorname{erf} \left(\sqrt{\frac{S_j}{2\sigma_{nj}^2}} \right) f_p \end{aligned} \quad (25)$$

with $f_p = 2p_T$ for random data without subcarrier and $|N_e| \leq N_s$, and

$f_p = f'_p = 2 \left(\frac{2N_s}{N_{sc}} - p_T \right)$ for random data plus subcarrier and $|N_e| \leq N_{sc}/2$.

Eq. (24) can be rewritten (using Eq. (18)) as

$$\bar{\epsilon}_n = G_Q \int_{t-T_c}^{t+T_R} N(t) dt \quad (26)$$

where

$$G_Q \triangleq \frac{G'_Q}{T_L} \quad (27)$$

Herein, G_Q will be treated as the "gain" of the cross-correlator-counter.

The variance of the error signal does not depend on the symbol transition rate and equals the sum of the variances in the upper and lower arms. Using Eq. (13), the variance at the output of the non-correlator counter will be

$$\begin{aligned} \sigma_{ej}^2 &= 2KN_s p_e (1 - p_e) / m_o^2 \\ &= \frac{KN_s}{2m_o^2} \left\{ 1 - \left[\operatorname{erf} \left(\sqrt{\frac{s_1}{2\sigma_{n1}^2}} \right) \operatorname{erf} \left(\sqrt{\frac{s_j}{2\sigma_{nj}^2}} \right) \right]^2 \right\} \end{aligned} \quad (28)$$

The above equation applies to random data, random data plus subcarrier, or a squarewave.

SECTION III

RTC LAPLACE TRANSFORM BLOCK DIAGRAM AND TRANSFER FUNCTION

The three basic components of the Real-Time Combiner are: cross-correlator-counter, loop filter and FIFO shifter. The transfer functions of these components are modelled as follows:*

Cross-Correlator-Counter

$$\frac{\epsilon(z)}{N_E(s)} \triangleq C(z, s) = G_Q \frac{1}{s} \frac{z-1}{z} \quad (29a)$$

Loop Filter

$$\frac{\Delta N(z)}{\epsilon(z)} \triangleq L(z) = \frac{z\Lambda}{z-R} \quad (29b)$$

FIFO

$$\frac{\hat{N}(s)}{\Delta N(z)} \triangleq F(z, s) = \frac{1-e^{-T_L s}}{s} \frac{z}{z-1} \quad (29c)$$

The time delay between the time instants that the error signal ϵ_n is read by the CPU and the delay update ΔN_n produced is modelled as

$$D(s) = e^{-gT_L s} \quad (30)$$

where $g \triangleq T_c/T_L$ is the ratio of computation time to loop update time. Although $D(s)$ is between the cross-correlator-counter and the loop filter, in order to obtain the equivalent block diagram in the z-domain we place $D(s)$ after the FIFO.

*The transfer functions are expressed as either z-transforms or hybrid s/z-transforms as appropriate, depending on whether the operation being performed is purely digital or a combination of analog and digital.

Combining Eqs. (27) through (30), the mixed mode Laplace block diagram of Figure 8 is obtained. The parameter G in this figure is the gain associate with delay rate compensation. Referring to Figure 8

$$X(s) = \frac{N(s)}{s} - Y(z) \left(1 - e^{-T_L s}\right) \frac{1}{s^2} e^{-gT_L s} \quad (31)$$

But since z corresponds to an update interval of T_L seconds, i.e., $z = e^{T_L s}$, then

$$1 - e^{-T_L s} = \frac{z-1}{z} \quad (32)$$

Thus,

$$X(s) = \frac{N(s)}{s} - \frac{1}{s^2} e^{-gT_L s} \Delta N(z) \quad (33)$$

where $\Delta N(z)$ is the z transform of the FIFO input. Taking the z -transform of Eq. (33), we obtain

$$X(z) = \left(\frac{N(s)}{s}\right)^* - \Delta N(z) \left(\frac{e^{-gT_L s}}{s^2}\right)^* \quad (34)$$

where the asterisk denotes the z -transform operation.

In general

$$\left[e^{-gT_L s} R(s) \right]^* \triangleq R(z, m), \quad m = 1-g \quad (35)$$

where $R(z, m)$ is the modified z -transform of $R(s)$. Using this property, Eq. (34) becomes

$$X(z) = \left(\frac{N(s)}{s}\right)^* - \Delta N(z) T_L \frac{z(1-g) + g}{(z-1)^2} \quad (36)$$

With this transformation, Figure 8 has the equivalent block diagram of Figure 9, which is entirely in the z -plane.

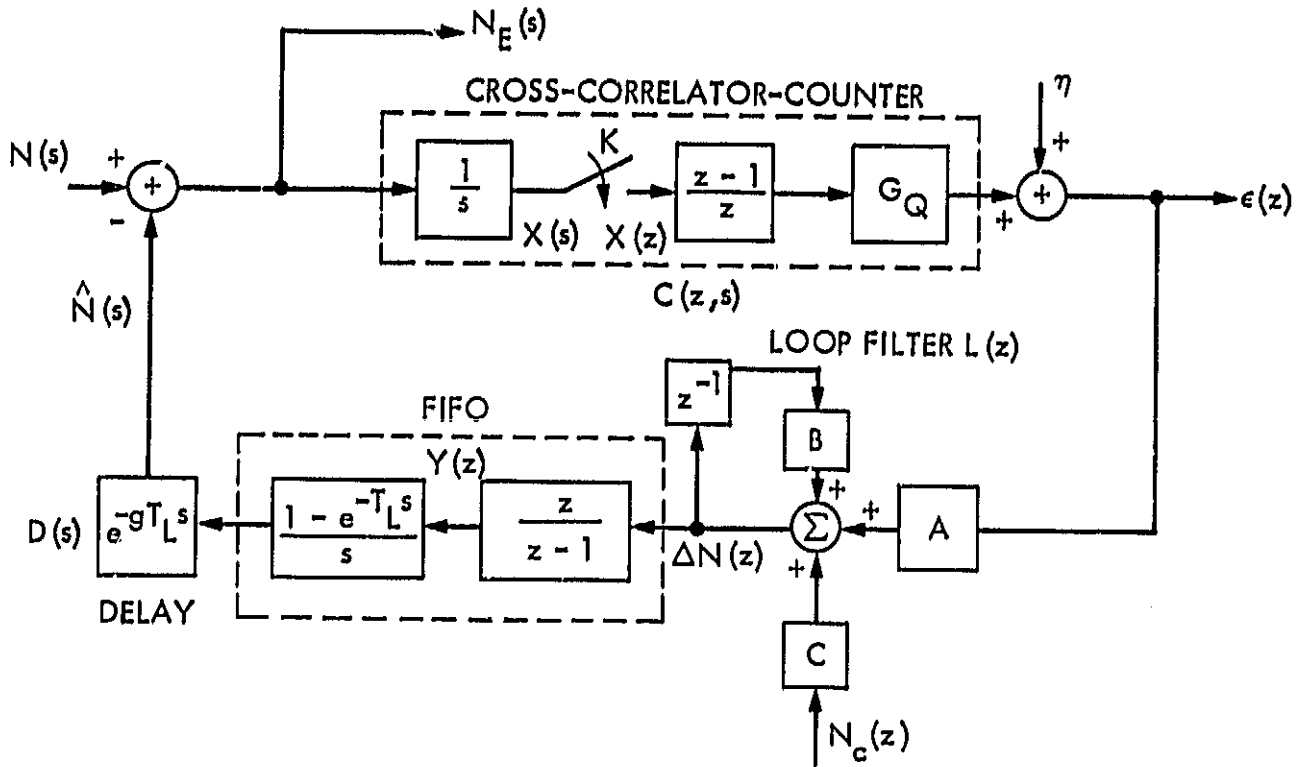


Figure 8. RTC Laplace Transform Block Diagram

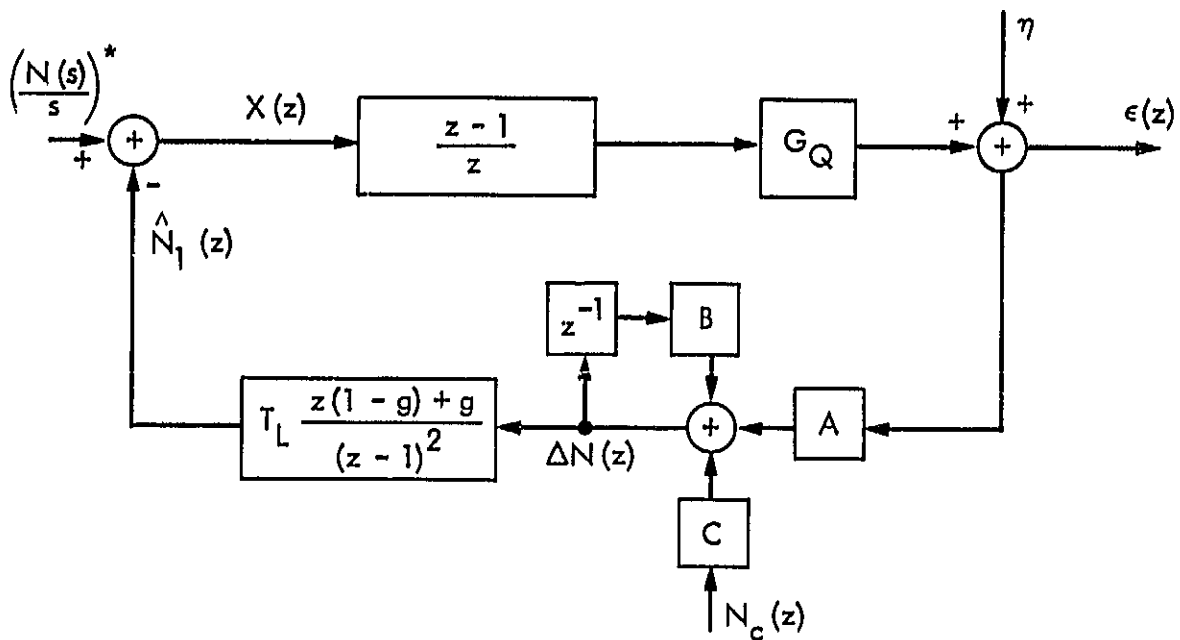


Figure 9. RTC Equivalent Block Diagram in z Domain

The open-loop transfer function for the RTC is

$$\frac{\hat{N}_1(z)}{X(z)} \triangleq G(z) = \frac{AG[z(1-g) + g]}{(z-1)(z-B)} \quad (37)$$

where G is the closed loop gain which for this configuration becomes identical with G'_Q as defined in Eq. (27). The closed-loop transfer function for the RTC is

$$\frac{\hat{N}_1(z)}{\left[\frac{N(s)}{s}\right]^*} \triangleq H(z) = \frac{G(z)}{1+G(z)} \quad (38)$$

or

$$H(z) = AG \frac{z(1-g) + g}{z^2 + z(AG(1-g) - B - 1) + B + gAG} \quad (39)$$

The denominator of Eq. (39) is the loop characteristic equation and has the root locus diagram as illustrated in Figure 10. Expressing it as

$$C(z) = z^2 + a_1z + a_0 \quad (40)$$

and solving for the gains A and B , we obtain

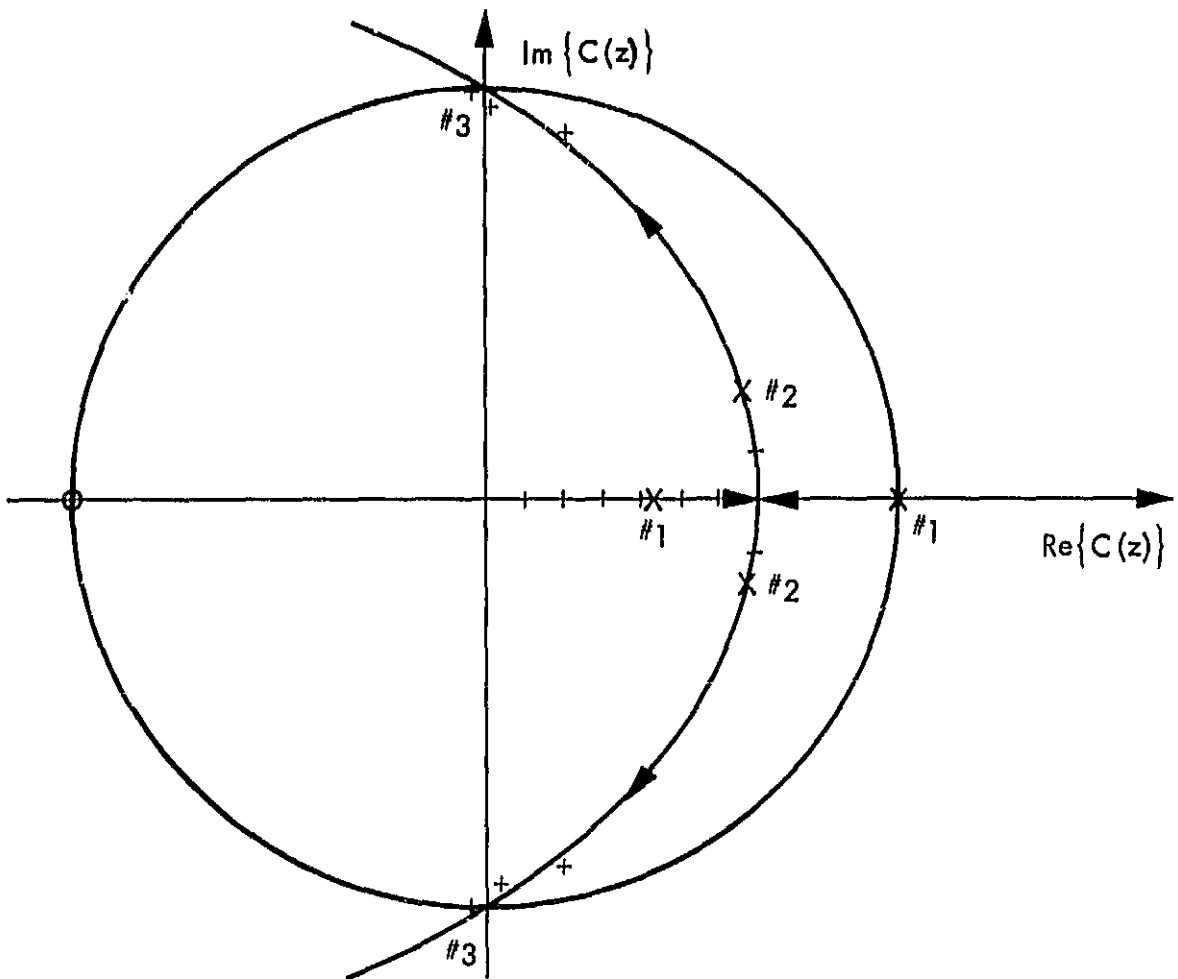
$$A = \frac{a_0 + a_1 + 1}{G} \quad (41)$$

$$B = a_0(1-g) - g(a_1+1) \quad (42)$$

For given values of damping factor ζ and settling time t_s , the natural frequency of the loop will be

$$\omega_n \approx \frac{4}{\zeta t_s} \quad (43)$$

The values for the constants a_0 and a_1 can be found from the following relation



- $g = 0.3$
- #1 - OPEN LOOP
- #2 - NOMINAL GAIN, $AG = 0.2374$
- #3 - $AG = 1.8$

Figure 10. Root Locus Diagram

$$a_1 = -2 e^{\zeta \omega_n T_L} \cos \left(\sqrt{1 - \zeta^2} \omega_n T_L \right) \quad (44)$$

$$a_0 = e^{-2\zeta \omega_n T_L} \quad (45)$$

where again T_L is the loop update time in seconds. This selection of a_0 , a_1 , and, consequently, the gains A and B will insure that the poles of the transfer function $H(z)$ will lie inside the unit circle and the loop will be stable. For example, by making $\zeta = 0.707$, $t_s = 9.5$ sec., and $T_L = 1.0$ sec., we get $a_0 = 0.4308$, $a_1 = -1.1934$, and the natural frequency $\omega_n = 0.6$ rad/sec. Also, the poles of $H(z)$ will be located at $0.5967 \pm j 0.2734$.

SECTION IV
NOISE ANALYSIS

The one-sided noise-equivalent bandwidth is defined as

$$B_L = \frac{1}{2T_L} \frac{1}{H^2(1)} \frac{1}{2\pi j} \oint \frac{dz}{z} H(z)H(z^{-1}) \quad (46)$$

Letting $z = 1$ in Eq. (39) gives $H^2(1) = 1$. Defining the integral I_2 as

$$I_2 = \frac{1}{2\pi j} \oint \frac{dz}{z} H(z)H(z^{-1}) , \quad (47)$$

we obtain

$$I_2 = A^2 G^2 \frac{((1-g)^2 + g^2)(1 + AGg + B) - 2(1-g)g(AG(1-g) - B - 1)}{(1 - (AGg + B)^2)(1 + AGg + B) - (1 - (AGg + B))(AG(1-g) - B - 1)^2} \quad (48)$$

The one-sided noise-equivalent bandwidth now becomes

$$B_L = \frac{1}{2T_L} I_2 \quad (49)$$

Table 1 gives B_L for selected values of AG and g . One can observe from these results that B_L is almost insensitive to the parameter g .

Referring to Figure 9, the open loop noise process η at the output of the cross-correlator-counter has zero mean and variance given by Eq. (28). We want to find the variance, σ_N^2 , of the closed loop delay error as a function of σ_ϵ^2 .

Assuming that the spectrum of the noise process, η , is wide in relation to the loop bandwidth, B_L , the closed-loop variance of the steady-state error signal will be

$$\sigma_{\epsilon_{SS}}^2 = \sigma_\epsilon^2 \left(\frac{1}{2\pi j} \oint H(z)H(z^{-1}) \frac{dz}{z} \right) \quad (50)$$

Table 1. Noise Equivalent Bandwidth in Hz vs. Loop Gain AG and Computation Time Factor g

Loop Gain AG	Computation Time Factor		
	g = 0.0	g = 0.3	g = 1.0
0.0001	4.4×10^{-5}	3.9×10^{-5}	3.1×10^{-5}
0.0010	4.4×10^{-4}	4.0×10^{-4}	3.1×10^{-4}
0.0100	4.4×10^{-3}	3.9×10^{-3}	3.2×10^{-3}
0.1000	4.6×10^{-2}	4.12×10^{-2}	3.7×10^{-2}
0.2374	0.1137	0.1058	0.1133
0.5000	0.2661	0.2630	0.4716
1.0000	0.6751	0.7851	----

where $H(z)$ is given by Eq. (39). Comparing Eq. (50) with Eq. (46), we see that the closed loop variance, $\sigma_{\epsilon_{SS}}^2$, can be expressed as a function of either B_L or I_2 . Since $H(1) = 1.0$, then

$$\sigma_{\epsilon_{SS}}^2 = \sigma_{\epsilon}^2 (2T_L B_L) = \sigma_{\epsilon}^2 I_2 \quad (51)$$

The closed loop variance, σ_N^2 , of the delay error is readily obtained from the steady-state closed-loop variance of the error signal, namely,

$$\sigma_N^2 = \frac{1}{(G_Q T_L)^2} \sigma_{\epsilon_{SS}}^2 \quad (52)$$

Combining Eqs. (25), (27), (28) and (51), and substituting the result in Eq. (52), we obtain, after much simplification, the desired result, namely the variance of the delay error in the j^{th} RTC, i.e.,

$$\sigma_{N_j}^2 = \frac{B_L T_L N_s}{K f_p^2} \left\{ \left[\operatorname{erf} \left(\sqrt{\frac{S_1}{2\sigma_{n1}^2}} \right) \operatorname{erf} \left(\sqrt{\frac{S_j}{2\sigma_{nj}^2}} \right) \right]^{-2} - 1 \right\} \quad (53)$$

SECTION V

DELAY RATE COMPENSATION

Referring to Figure 8, we want to find the value for the gain C such that when an estimated delay rate compensation is applied at the input of C, the expected value of the error signal is zero. The estimated delay rate can be expressed as

$$n_c(t) = (\dot{n} + \Delta\dot{n}) u(t) \quad (54)$$

where $u(t)$ is the unit step function, \dot{n} is the actual delay rate of the input signal and $\Delta\dot{n}$ is the error made in estimating \dot{n} . Neglecting for the moment the noise process n , the state equation of the RTC loop is

$$\begin{pmatrix} N_{i+1} \\ \Delta N_{i+1} \end{pmatrix} = \begin{pmatrix} 1 - AG & -AGg - B \\ AG & AGg + B \end{pmatrix} \begin{pmatrix} N_i \\ \Delta N_i \end{pmatrix} + \begin{pmatrix} (T_L - Ac(1 - 2g) - C) & -C \\ (Ac(1 - 2g) + C) & C \end{pmatrix} \begin{pmatrix} \dot{n} \\ \Delta\dot{n} \end{pmatrix} \quad (55)$$

where N_i is the delay error at time i , ΔN_i is the delay update at time i

and $c \triangleq GT_L/2$.

In the steady state ($i \rightarrow \infty$), we want

$$N = -\frac{\Delta N}{2} \quad (56)$$

Inserting Eq. (56) into Eq. (55) and solving for N, we get:

$$N = -\frac{T_L \dot{n}}{2} \quad (57)$$

Inserting now Eq. (57) in the upper or lower row of Eq. (55) and solving for C, we get the expression for the doppler compensation gain, namely,

$$C = T_L(1 - B) \quad (58)$$

Note that the gain C is independent of the computation time.

Taking the z -transform of $N(s)/s$, the steady state error due to an input delay ramp when $n_c(t) = 0$ is

$$\begin{aligned}\bar{e}_{ss1} &= \lim_{z \rightarrow 1} \left(\frac{\dot{n}T_L^2 z(z+1)}{2(z-1)^3} \right) \left(\frac{z-1}{z} \right) \frac{G_Q(z-1)}{z[1+G(z)]} \\ &= \frac{\dot{n}T_L(1-B)}{A}\end{aligned}\quad (59)$$

Using Eq. (38) when $N(s)/s = 0$ and taking the z -transform of Eq. (54), the steady state error due to delay rate compensation $n_c(t)$ is

$$\begin{aligned}\bar{e}_{ss2} &= \lim_{z \rightarrow 1} \left[(\dot{n} + \Delta\dot{n}) \frac{z}{z-1} \right] \left(\frac{z-1}{z} \right) \frac{(-C)G(z(1-g) + g)}{(z-1)(z-B)[1+G(z)]} \\ &= -(\dot{n} + \Delta\dot{n}) \frac{C}{A}\end{aligned}\quad (60)$$

Substituting Eq. (58) into Eq. (60) and using Eq. (59), we get the total steady state error

$$\begin{aligned}\bar{e}_{ss} &= \bar{e}_{ss1} + \bar{e}_{ss2} \\ &= \frac{\dot{n}T_L(1-B)}{A} - \frac{\dot{n}T_L(1-B)}{A} - \frac{\Delta\dot{n}T_L(1-B)}{A} \\ &= -\frac{\Delta\dot{n}T_L(1-B)}{A}\end{aligned}\quad (61)$$

Since $E\{\Delta\dot{n}\} = 0$, the steady state error has zero expected value, as desired.

SECTION VI
OPTIMUM COHERENT COMBINING

In this section, we determine the optimum weighting factors, α_i ; $i = 1, 2, \dots, L$, such that the SNR at the combiner's output is maximized (see Figure 3). Referring to Figure 11, coherent signal combining implies that the amplitudes of the signals add coherently. This means that at the combiner output

$$\sqrt{S_A} = \mathbb{E} \left\{ \sqrt{S_{A1}} \right\} = \mathbb{E} \left\{ \sum_{j=1}^L \alpha_j s_{ji} \right\} = \sum_{j=1}^L \alpha_j \sqrt{S_j} \quad (62)$$

where s_{ij} = the signal amplitude of the i^{th} sample of the j^{th} signal = $\sqrt{S_j}$ on the average, α_j = the weighting factor for the j^{th} signal, and L = the number of signals combined.

The noise processes in each of the channels are statistically independent. As a result, their powers add, i.e., the noise power of the i^{th} sample at the combiner's output is equal to the weighted sum of the noise powers at the input. Hence,

$$N_A = \mathbb{E} \left\{ \sum_{j=1}^L \alpha_j^2 n_{ji}^2 \right\} = \sum_{j=1}^L \alpha_j^2 \sigma_{nj}^2 \quad (63)$$

where $\sigma_{nj}^2 = \mathbb{E}\{n_{ji}^2\}$ is the rms noise amplitude squared in the j^{th} channel.

The SNR at the output of the signal combiner for an arbitrary set of weighting factors is

$$R = \frac{\left[\sum_{j=1}^L \alpha_j \sqrt{S_j} \right]^2}{\sum_{j=1}^L \alpha_j^2 \sigma_{nj}^2} \quad (64)$$

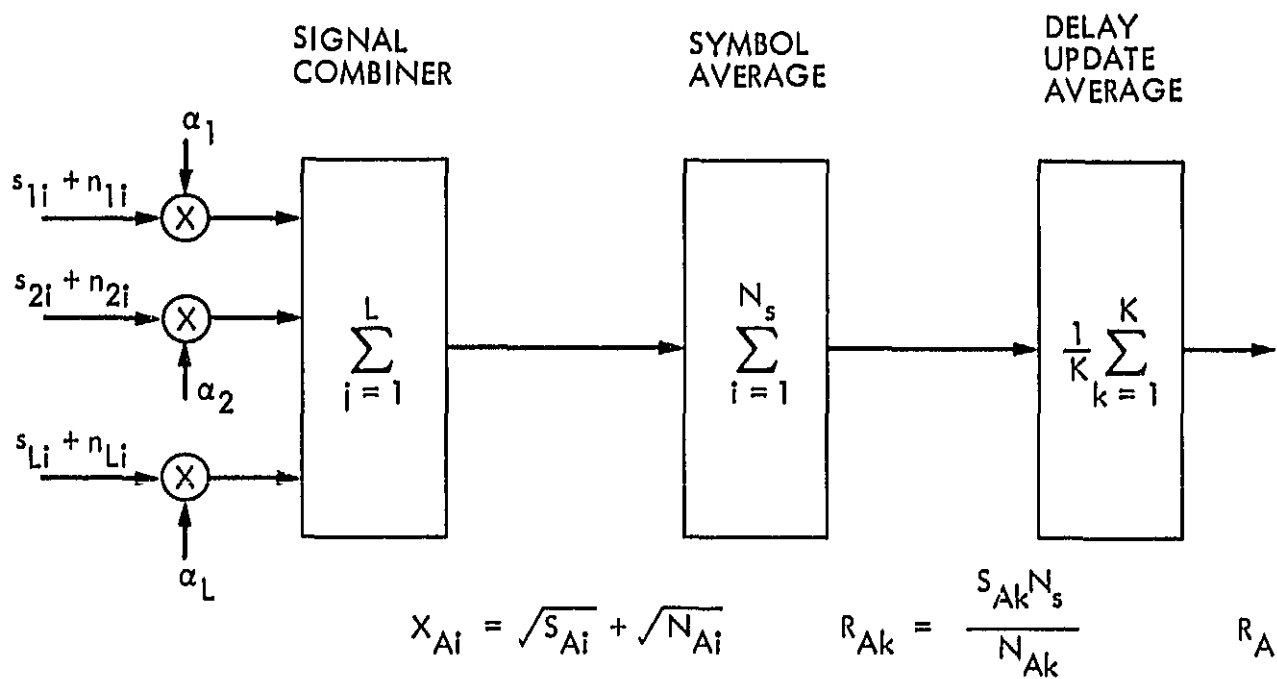


Figure 11. BBA Signal Combiner Model.

Given a set of signal amplitudes, $\sqrt{S_j}$, and rms noise amplitudes, $\{\sigma_{nj}\}$, at the combiner's input, then $\{\alpha_j\}$ is chosen so as to maximize the parameter R of Eq. (64). Differentiating R with respect to each of the weighting factors and equating the results to zero, i.e.,

$$\frac{\partial R}{\partial \alpha_j} = 0 \quad \text{for } j = 1, \dots, L \quad (65)$$

provides the solution

$$\alpha_j = \frac{\sqrt{S_j}}{\sigma_{nj}} \left(\frac{N_A}{\sqrt{S_A}} \right) \quad (66)$$

Since the common factor $N_A/\sqrt{S_A}$ does not affect the combiner output SNR, it can be set to any arbitrary value, e.g., unity. This, the equivalent choice of weighting coefficients, is

$$\alpha_j = \frac{\sqrt{S_j}}{\sigma_{nj}} \quad (67)$$

This optimization assumes that there are no delay errors at the input to the combiner, i.e., the BBA's tracking loops are functioning ideally.

SECTION VII

DEGRADATION OF THE SUMMER OUTPUT SIGNAL-TO-NOISE RATIO

(SNR) DUE TO DELAY JITTER

For an arbitrary set of weighting coefficients, $\{\alpha_j\}$; $j = 1, 2, \dots, L$, the output of the combiner, as shown in Figure 11, is given by

$$X_{A1} = \sqrt{S_{A1}} + \sqrt{N_{A1}} = \sum_{j=1}^L \alpha_j s_{j1} + \sum_{j=1}^L \alpha_j n_{j1}; \quad i = 1, 2, \dots, N_B \quad (68)$$

where $j = 1$ refers to the reference channel whose signal is assumed to have no timing error. Adding all of the X_{A1} samples over the k^{th} symbol interval, the output of the combiner is

$$\begin{aligned} \bar{X}_{Ak} &= \sum_{i=1}^{N_B} X_{A1} = \sum_{i=1}^{N_B} \left(\sqrt{S_{A1}} + \sqrt{N_{A1}} \right) \\ &= \sum_{j=1}^L \alpha_j \sqrt{S_j} (N_B - (4n + 1) |\delta_{jk}|) + \sum_{j=2}^L \alpha_j b_j \sqrt{S_j} |\delta_{jk}| + \sqrt{N_{Ak}} \\ &= \sqrt{S_A} N_B - \sum_{j=2}^L \alpha_j \sqrt{S_j} |\delta_{jk}| (4n - b_j + 1) + \sqrt{N_{Ak}} \end{aligned} \quad (69)$$

where, as before, $n = N_B/N_{sc}$ = the ratio of the data period to the subcarrier period, K = the number of symbols between delay updates, and δ_{jk} = the delay error (number of samples) in the j^{th} channel during the k^{th} symbol with respect to the reference (1^{st}) channel. By definition, $\delta_{1k} = 0$ for all $k = 1, 2, \dots, K$.

The quantity $\sqrt{N_{Ak}}$ is the noise at the combiner output over the interval of one (the k^{th}) symbol. It represents the noise effects from all channels. It is modelled as a Gaussian random variable with zero mean and variance

$$\sigma_k^2 = \sum_{j=1}^L \alpha_j^2 \sigma_{nj}^2 N_s = N_A N_s \quad (70)$$

Furthermore, b_j represents random data from adjacent symbols, which takes on values ± 1 with equal probability. Thus,

$$\begin{aligned}\mathbb{E} \left\{ (4n - b_j + 1) \right\} &= 4n + 1 \triangleq u \\ \mathbb{E} \left\{ (4n + 1 - b_j)^2 \right\} &= (4n)^2 + 8n + 2 \triangleq w\end{aligned}\quad (71)$$

It is assumed that each delay error δ_{jk} can be modelled as a Gaussian random variable with mean

$$\bar{\delta}_{jk} = \bar{N}_j + \dot{n}_j k \quad (72)$$

and variance

$$\begin{aligned}\sigma_{\delta_{jk}}^2 &= \mathbb{E} \left\{ \left[N_j + \dot{n}_j k - (\bar{N}_j + \dot{n}_j k) \right]^2 \right\} \\ &= \mathbb{E} \left\{ (N_j - \bar{N}_j)^2 \right\} = \sigma_{N_j}^2\end{aligned}\quad (73)$$

Here $\sigma_{N_j}^2$ is the variance of the delay error at delay update instants and is given by Eq. (53). Also, \dot{n}_j denotes the delay rate of the j^{th} signal in units of samples per symbol.

Since we have assumed that the delay error is a Gaussian random variable, the probability density function of the absolute value of the delay error will be

$$P(|\delta_{jk}|) = \frac{1}{\sqrt{2\pi} \sigma_{\delta_{jk}}} \left[\exp \left(-\frac{(\delta_{jk} - \bar{\delta}_{jk})^2}{2 \sigma_{\delta_{jk}}^2} \right) + \exp \left(-\frac{(\delta_{jk} + \bar{\delta}_{jk})^2}{2 \sigma_{\delta_{jk}}^2} \right) \right] u(\delta_{jk}) \quad (74)$$

with mean

$$\begin{aligned}\bar{\Delta}_{jk} \triangleq \mathbb{E}\{|\delta_{jk}|\} &= \left[\sqrt{\frac{2}{\pi}} \sigma_{\delta_{jk}} \left(e^{-a^2} - \frac{e^{-b^2} + e^{-c^2}}{2} \right) + \bar{\delta}_{jk} \operatorname{erf}(a) \right. \\ &\quad \left. + \frac{\bar{\delta}_{jk}}{2} (\operatorname{erf}(b) - \operatorname{erf}(c)) \right] \frac{1}{d_{jk}}\end{aligned}\quad (75)$$

where

$$\begin{aligned}
 a &= \frac{\bar{\delta}_{jk}}{\sqrt{2 \sigma_{\delta_{jk}}^2}}, & b &= \frac{N_s - \bar{\delta}_{jk}}{\sqrt{2 \sigma_{\delta_{jk}}^2}}, \\
 c &= \frac{N_s + \bar{\delta}_{jk}}{\sqrt{2 \sigma_{\delta_{jk}}^2}}, & d_{jk} &= \frac{1}{2} (\text{erf}(b) + \text{erf}(c))
 \end{aligned} \tag{76}$$

Here, $\bar{\delta}_{jk}$ and $\sigma_{\delta_{jk}}^2$ are defined by Eqs. (72) and (73), respectively.

The expected value of $|\delta_{jk}|^2 \triangleq \bar{\Delta}_{jk}^2$ will be

$$\begin{aligned}
 \bar{\Delta}_{jk}^2 &= \left\{ \sigma_{\delta_{jk}}^2 + (\bar{\delta}_{jk})^2 - \left[\frac{1}{\sqrt{\pi}} \sigma_{\delta_{jk}}^2 \left(be^{-b^2} + ce^{-c^2} \right) \right. \right. \\
 &\quad \left. \left. + \sqrt{\frac{2}{\pi}} \sigma_{\delta_{jk}}^2 \left(e^{-b^2} - e^{-c^2} \right) \right] \frac{1}{d_{jk}} \right\}
 \end{aligned} \tag{77}$$

Assuming zero differential doppler, i.e., $\dot{n}_j = 0$ for all j ,

$$a = 0, \quad b = c = \frac{N_s}{\sqrt{2 \sigma_{N_j}}}, \quad d_{jk} = \text{erf} \left(\frac{1}{p_j \sqrt{2}} \right) \tag{78}$$

where

$$p_j \triangleq \frac{\sigma_{N_j}}{N_s} \tag{79}$$

and Eqs. (75) and (77) reduce to

$$\bar{\Delta}_{jk} \triangleq \bar{\Delta}_j = \sqrt{\frac{2}{\pi}} \sigma_{N_j} \left(1 - e^{-1/2 p_j^2} \right) \frac{1}{\text{erf} \left(\frac{1}{p_j \sqrt{2}} \right)} \tag{80}$$

ORIGINAL VERSION
OF POOR QUALITY

$$\overline{\Delta_{jk}^2} \triangleq \overline{\Delta_j^2} = \sigma_{N_j}^2 \left(1 - \sqrt{\frac{2}{\pi}} \left(\frac{1}{p_j} \right) \frac{e^{-1/2 p_j^2}}{\operatorname{erf} \left(\frac{1}{p_j \sqrt{2}} \right)} \right) \quad (81)$$

Note that as $1/p_j$ approaches zero,

$$\begin{aligned} \overline{\Delta_j} &\rightarrow \frac{N_s}{2} \\ \overline{\Delta_j^2} &\rightarrow \frac{N_s^2}{2} \end{aligned} \quad (82)$$

and for $1/p_j$ that is very large,

$$\begin{aligned} \overline{\Delta_j} &\rightarrow \sqrt{\frac{2}{\pi}} \sigma_{N_j} \\ \overline{\Delta_j^2} &\rightarrow \sigma_{N_j}^2 \end{aligned} \quad (83)$$

The SNR at the output of the combiner averaged over the interval of one delay update period is given by

$$R_A = \frac{\mathbb{E} \left\{ \left[\frac{1}{K} \sum_{k=1}^K \left(\sum_{j=1}^L \alpha_j \sqrt{S_j} N_s - \sum_{j=2}^L \alpha_j \sqrt{S_j} |\dot{\phi}_{jk}| (4n + 1 - b_j) \right) \right]^2 \right\}}{\frac{1}{K} \sum_{k=1}^K \sigma_k^2} \quad (84)$$

To compute the SNR of the combiner's output, only the case of the zero differential doppler will be considered. For this case, both the numerator and denominator of Eq. (84) are not functions of k . Hence, Eq. (84) simplifies to

$$R_A = \frac{\mathbb{E} \left\{ \left(\sum_{j=1}^L \alpha_j \sqrt{S_j} N_s - \sum_{j=2}^L \alpha_j \sqrt{S_j} |\dot{\phi}_j| (4n + 1 - b_j) \right)^2 \right\}}{N_A N_s} \quad (85)$$

Expanding the numerator of the above equation, we obtain

$$S_A N_s^2 - 2 \mathbb{E} \left\{ \sum_{j=2}^L \alpha_j \sqrt{S_j} (4n + 1 - b_j) |\delta_j| \right\} \sqrt{S_A} N_s + \mathbb{E} \left\{ \left[\sum_{j=2}^L \alpha_j \sqrt{S_j} (4n + 1 - b_j) |\delta_j| \right]^2 \right\} \quad (86)$$

Evaluating the expectations as required in Eq. (86) gives

$$S_A N_s^2 - 2u \sqrt{S_A} N_s \sum_{j=2}^L \alpha_j \sqrt{S_j} \bar{\Delta}_j + w \sum_{j=2}^L \alpha_j^2 S_j \overline{\Delta_j^2} + \left(u \sum_{j=2}^L \alpha_j \sqrt{S_j} \bar{\Delta}_j \right)^2 - u^2 \sum_{j=2}^L \alpha_j^2 S_j (\bar{\Delta}_j)^2 \quad (87)$$

where $\bar{\Delta}_j$ and $\overline{\Delta_j^2}$ are defined by Eqs. (80) and (81), respectively, and u and w are defined by Eq. (71). Using these results, the SNR at the output of the combiner will be

$$R_A = \frac{S_A N_s}{N_A} \left[1 - \left(2u \sum_{j=2}^L \alpha_j \frac{\sqrt{S_j} \bar{\Delta}_j}{\sqrt{S_A} N_s} - w \sum_{j=2}^L \alpha_j^2 \frac{S_j \overline{\Delta_j^2}}{S_A N_s^2} + u^2 \sum_{j=2}^L \alpha_j^2 \frac{S_j (\bar{\Delta}_j)^2}{S_A N_s^2} - \left(u \sum_{j=2}^L \alpha_j \frac{\sqrt{S_j} \bar{\Delta}_j}{\sqrt{S_A} N_s} \right)^2 \right) \right] = \frac{S_A N_s}{N_A} D \quad (88)$$

where

$$D \triangleq 1 - \Delta \quad (89)$$

is a degradation factor representing the reduction in output SNR from its value $S_A N_s / N_A$ when there is no delay error. Hence, at zero delay errors, $D = 1$. The variation about $D = 1$ is given by

$$\Delta = 2u \sum_{j=2}^L \alpha_j \frac{\sqrt{s_j} \bar{\Delta}_j}{\sqrt{s_A} N_s} - w \sum_{j=2}^L \alpha_j^2 \frac{s_j \bar{\Delta}_j^2}{s_A N_s^2} + u^2 \sum_{j=2}^L \alpha_j^2 \frac{s_j (\bar{\Delta}_j)^2}{s_A N_s^2} - \left(u \sum_{j=2}^L \alpha_j \frac{\sqrt{s_j} \bar{\Delta}_j}{\sqrt{s_A} N_s} \right)^2 \quad (90)$$

The above expression is valid for an arbitrary set of $\{\alpha_j\}$. If the optimum values are substituted from Eq. (66), then Δ_{opt} is

$$\Delta_{opt} = 2u \sum_{j=2}^L \left(\frac{s_j}{s_A} \right) \left(\frac{N_A}{\sigma_{nj}^2} \right) \left(\frac{\bar{\Delta}_j}{N_s} \right) - w \sum_{j=2}^L \left(\frac{s_j}{s_A} \right)^2 \left(\frac{N_A}{\sigma_{nj}^2} \right)^2 \left(\frac{\bar{\Delta}_j^2}{N_s^2} \right) + u^2 \sum_{j=2}^L \left(\frac{s_j}{s_A} \right)^2 \left(\frac{N_A}{\sigma_{nj}^2} \right)^2 \left(\frac{\bar{\Delta}_j}{N_s} \right)^2 - \left(u \sum_{j=2}^L \left(\frac{s_j}{s_A} \right) \left(\frac{N_A}{\sigma_{nj}^2} \right) \left(\frac{\bar{\Delta}_j}{N_s} \right) \right)^2 \quad (91)$$

Assuming

$$s_j = \frac{s_1}{4}, \quad \sigma_{nj}^2 = \sigma_{n1}^2 \quad \text{for } j = 2, \dots, L \quad (92)$$

then the optimum weighting factors can be specified as

$$\alpha_1 = 2, \quad \alpha_j = 1 \quad \text{for } j = 2, \dots, L \quad (93)$$

Under the above assumptions

$$\frac{s_j}{s_A} = \left(\frac{1}{L+3} \right)^2 \quad (94a)$$

$$\frac{N_A}{\sigma_{nj}^2} = L+3 \quad (94b)$$

$$\left(\frac{S_j}{S_A}\right) \left(\frac{N_A}{\sigma_{n_j}^2}\right) = \frac{1}{L+3} \quad \text{for } j = 2, \dots, L \quad (94c)$$

Finally, it can be assumed that the rms delay errors in all tracking loops are identical, i.e.,

$$\sigma_{N_j} = \sigma_N \quad \text{for } j = 2, \dots, L \quad (95)$$

and furthermore,

$$p_j = p \quad \text{for } j = 2, 3, \dots, L \quad (96)$$

Making all of these substitutions in Eq. (91) gives the simplified result

$$\begin{aligned} \Delta_{\text{opt}} = & 2u \sqrt{\frac{2}{\pi}} \frac{L-1}{L+3} p r_\sigma - w \frac{L-1}{(L+3)^2} p \left(p - \sqrt{\frac{2}{\pi}} \frac{e^{-1/2p^2}}{\text{erf}\left(\frac{1}{p\sqrt{2}}\right)} \right) \\ & + u^2 \frac{2}{\pi} \frac{L-1}{(L+3)^2} p^2 r_\sigma^2 - u^2 \frac{2}{\pi} \left(\frac{L-1}{L+3} p r_\sigma \right)^2 \end{aligned} \quad (97)$$

where

$$r_\sigma \triangleq \left(1 - e^{-1/2p^2} \right) \frac{1}{\text{erf}\left(\frac{1}{p\sqrt{2}}\right)} \quad (98)$$

The SNR degradation from ideal performance is given by

$$D_{\text{opt}} = 1 - \Delta_{\text{opt}} \quad (99)$$

Using Eqs. (97) and (99), and the above assumptions, the SNR degradation D_{opt} at the combiner output is plotted in Figures 12 through 17 versus the input symbol SNR of the reference channel for parameter values typical of the Voyager, Pioneer, and Venus Radar Mapper (VRM) missions.

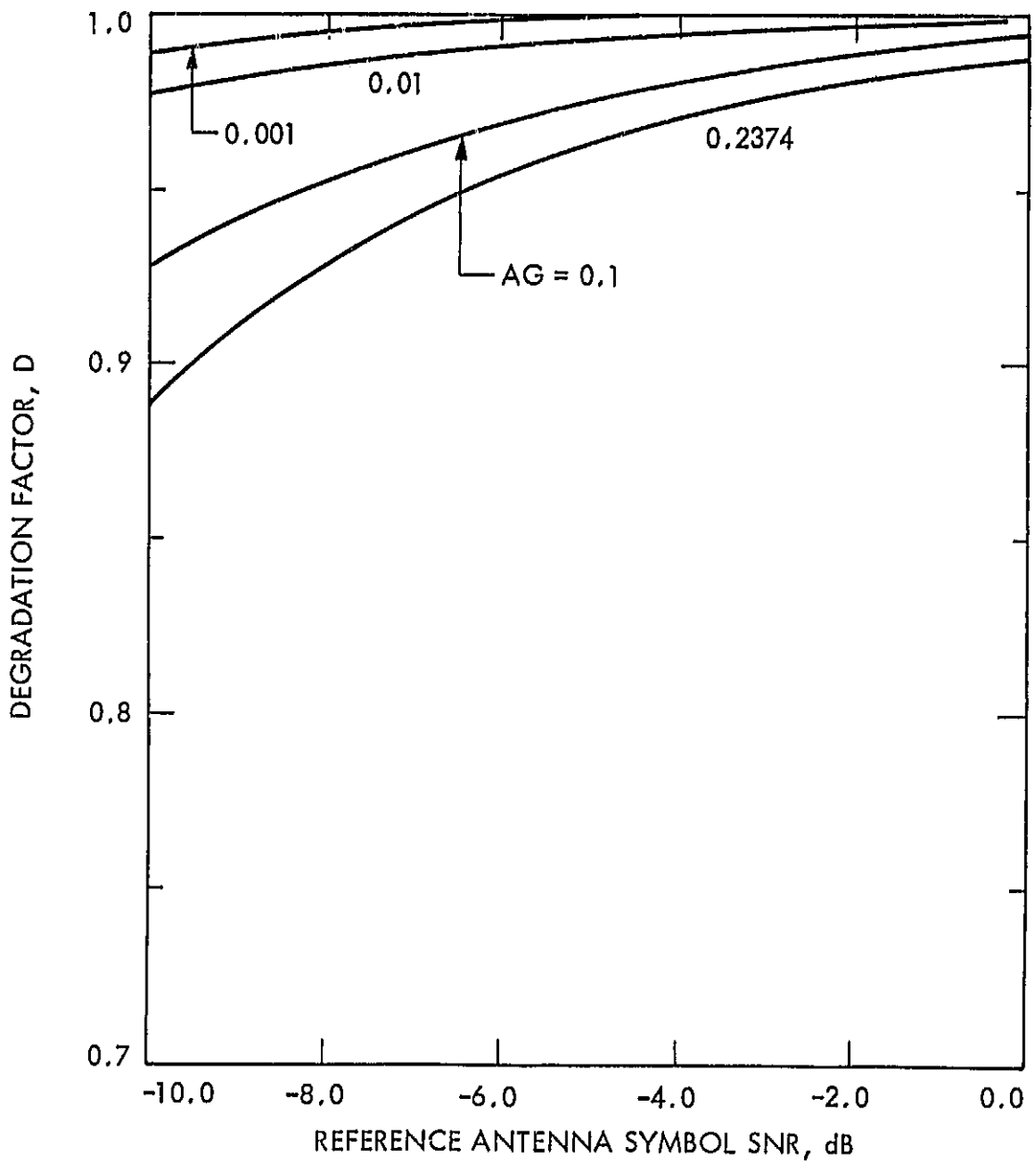


Figure 12. Degradation Factor vs. Symbol SNR, Voyager Mission, $L = 2$. Other conditions include: noise bandwidth (B_n) = 3.75×10^6 Hz, symbol rate (r) = 40×10^3 symbols per second (sps), subcarrier frequency = 360×10^3 Hz, integration time = 1 second, $g = 0.3$, and $S_i = S_1/4$; $i = 2, \dots, L$.

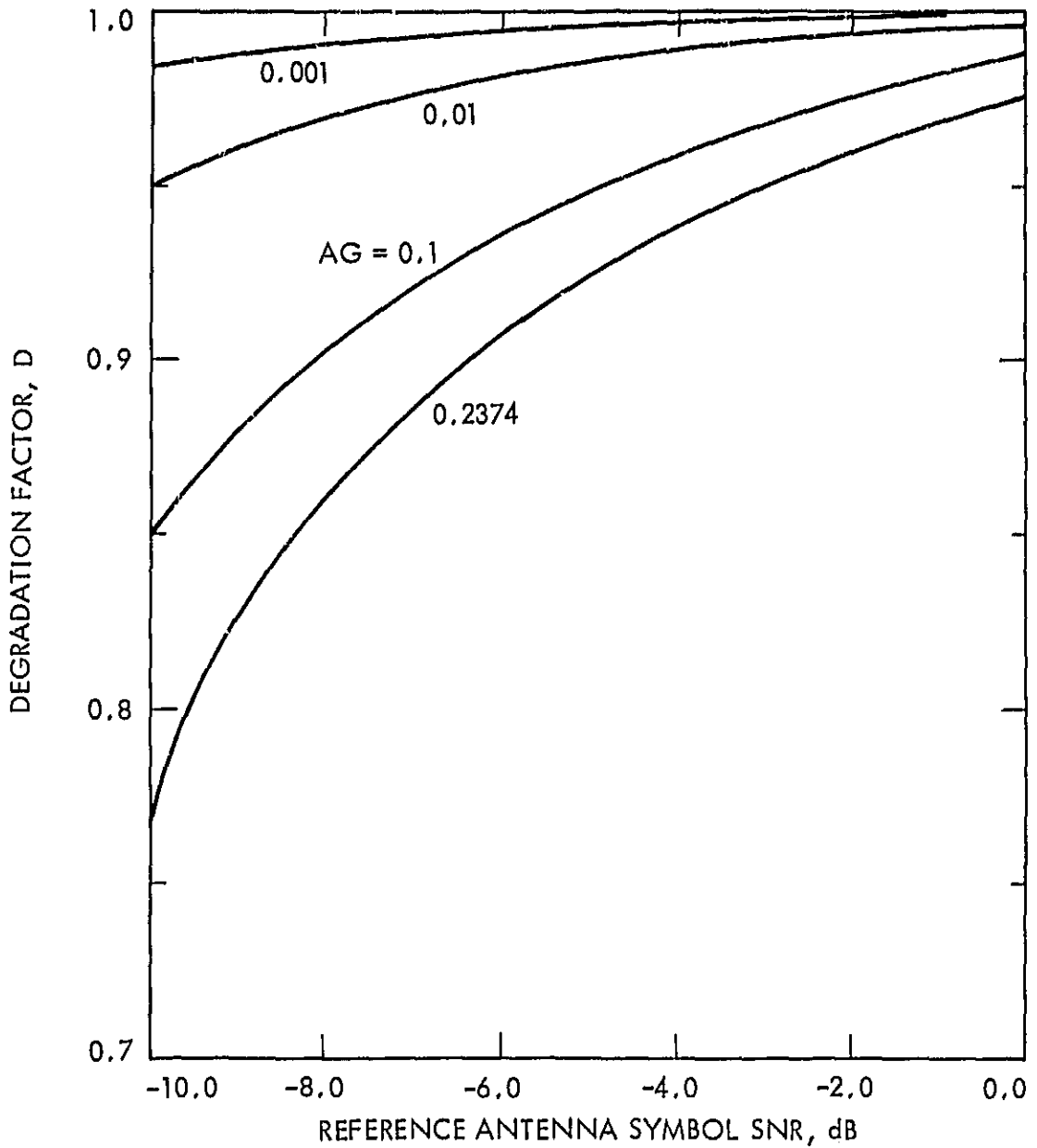


Figure 13. Degradation Factor vs. Symbol SNR, Voyager Mission, $L = 4$. Other conditions include: noise bandwidth (B_{fl}) = 3.75×10^6 Hz, symbol rate (r) = 40×10^3 sps, subcarrier frequency = 360×10^3 Hz, integration time = 1 second, $g = 0.3$, and $S_i = S_1/4$; $i = 2, \dots, L$.

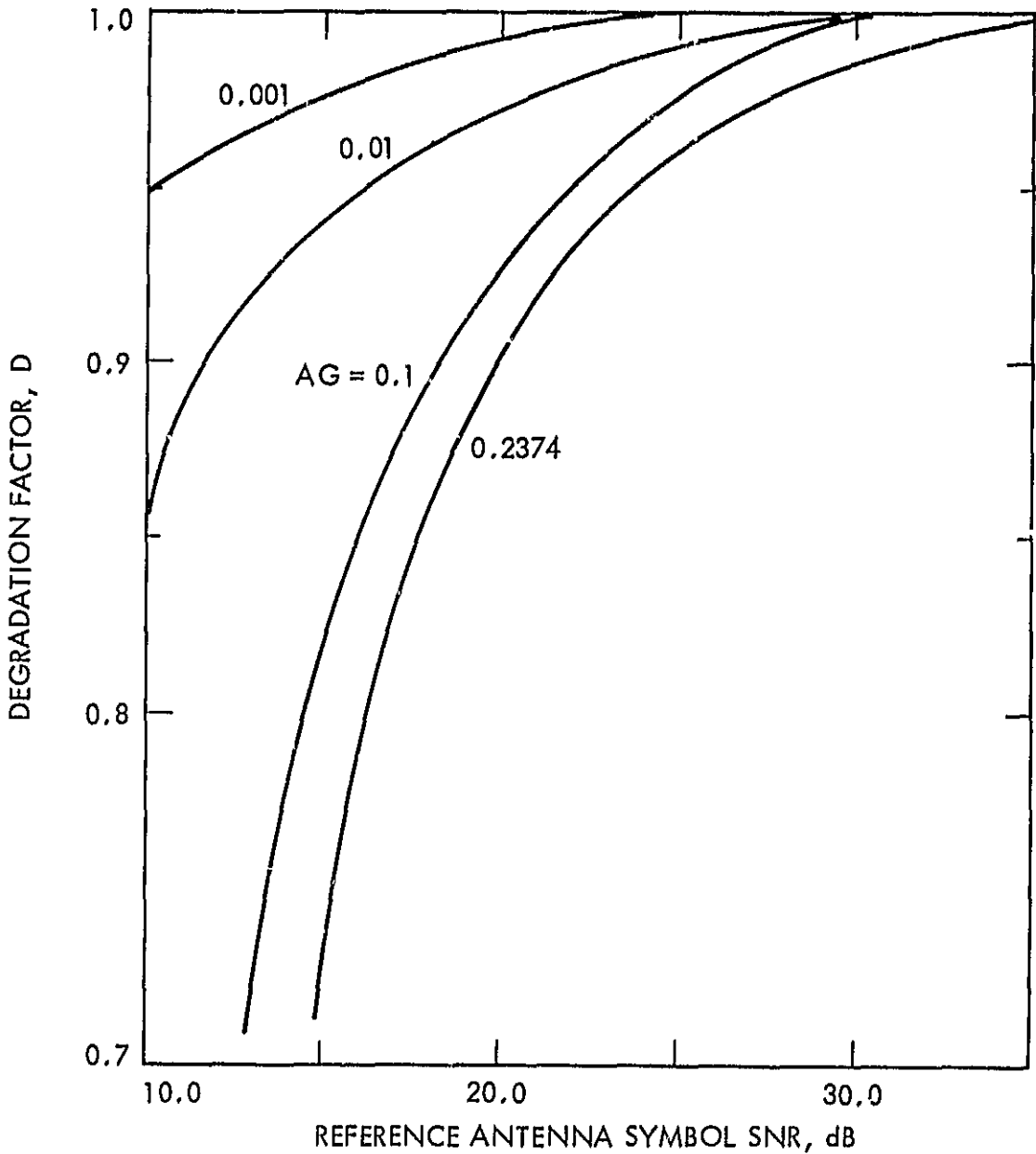


Figure 14. Degradation Factor vs. Symbol SNR, Pioneer Mission, $L = 2$. Other conditions include: noise bandwidth (B_n) = 135×10^3 Hz, symbol rate (r) = 8 sps, subcarrier frequency = 2×10^3 Hz, integration time = 1 second, $g = 0.3$, and $S_i = S_1/4$; $i = 2, \dots, L$.

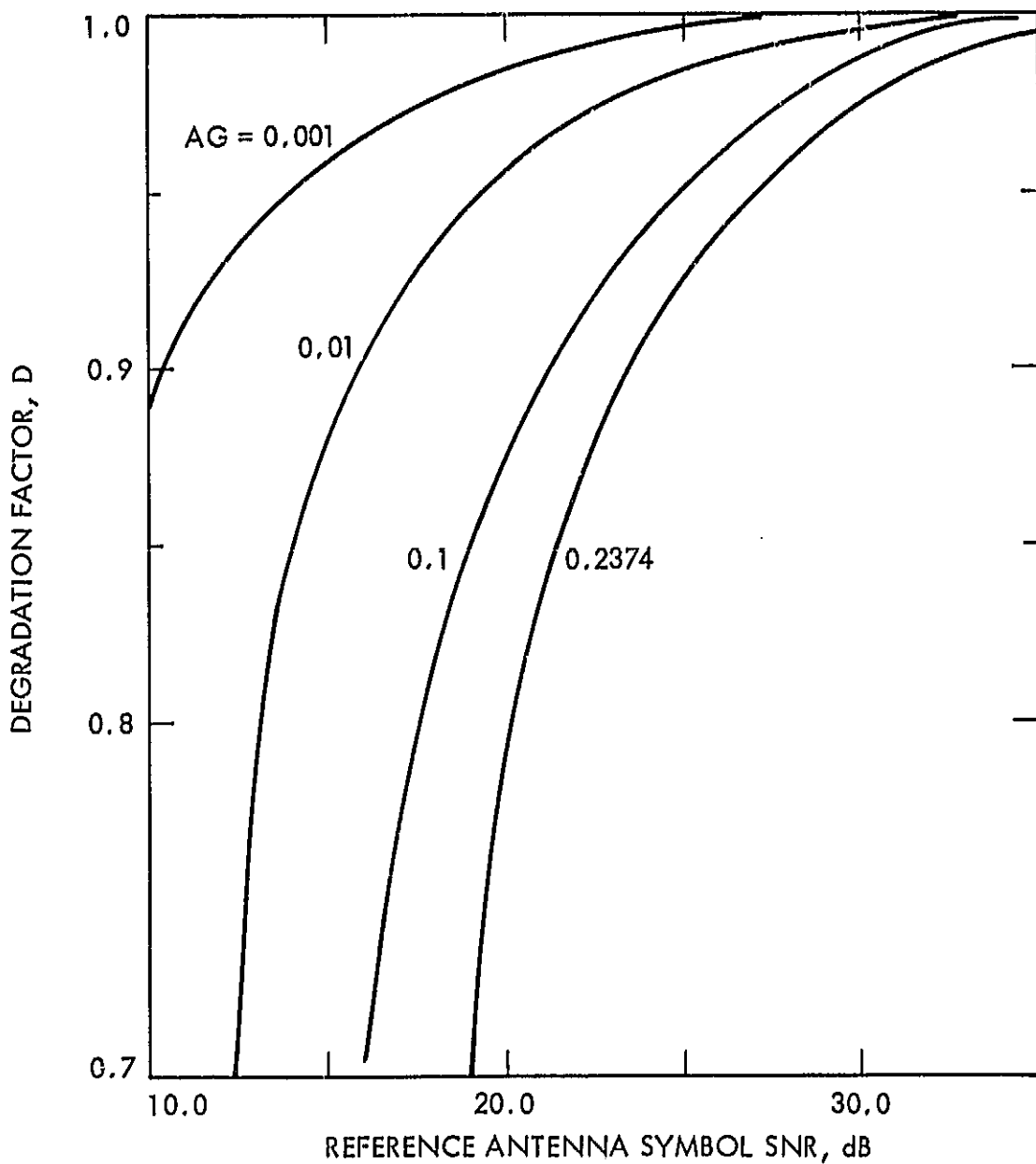


Figure 15. Degradation Factor vs. Symbol SNR, Pioneer Mission, $L = 4$. Other conditions include: noise bandwidth (B_n) = 135×10^3 Hz, symbol rate (r) = 8 sps, subcarrier frequency = 2×10^3 Hz, integration time = 1 second, $g = 0.3$, and $S_i = S_1/4$; $i = 2, \dots, L$.

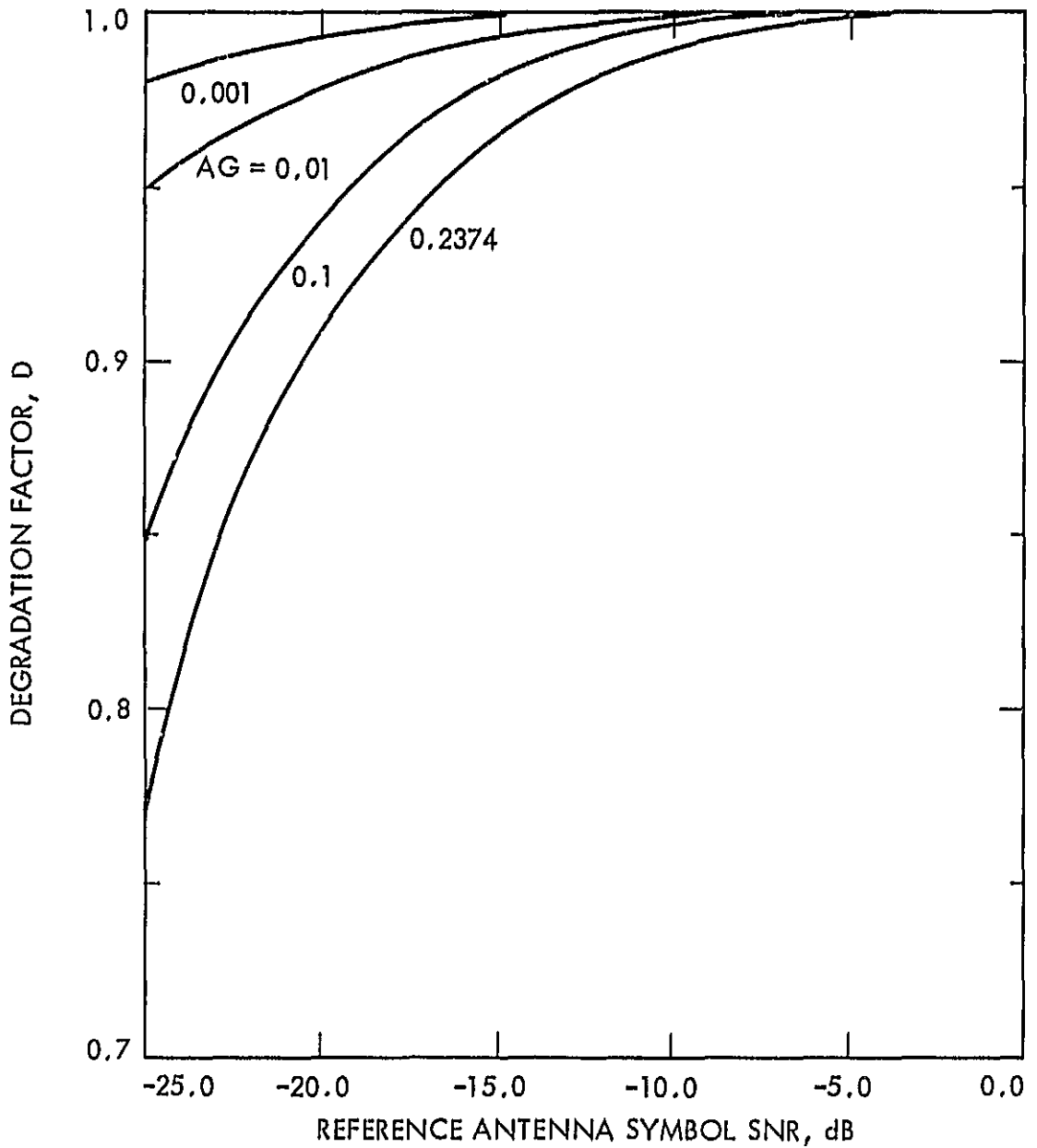


Figure 16. Degradation Factor vs. Symbol SNR, VRM Mission, $L = 2$. Other conditions include: noise bandwidth (B_n) = 3.75×10^6 Hz, symbol rate (r) = 550×10^3 sps, subcarrier frequency = 900×10^3 Hz, integration time = 1 second, $g = 0.3$, and $S_i = S_1/4$; $i = 2, \dots, L$.

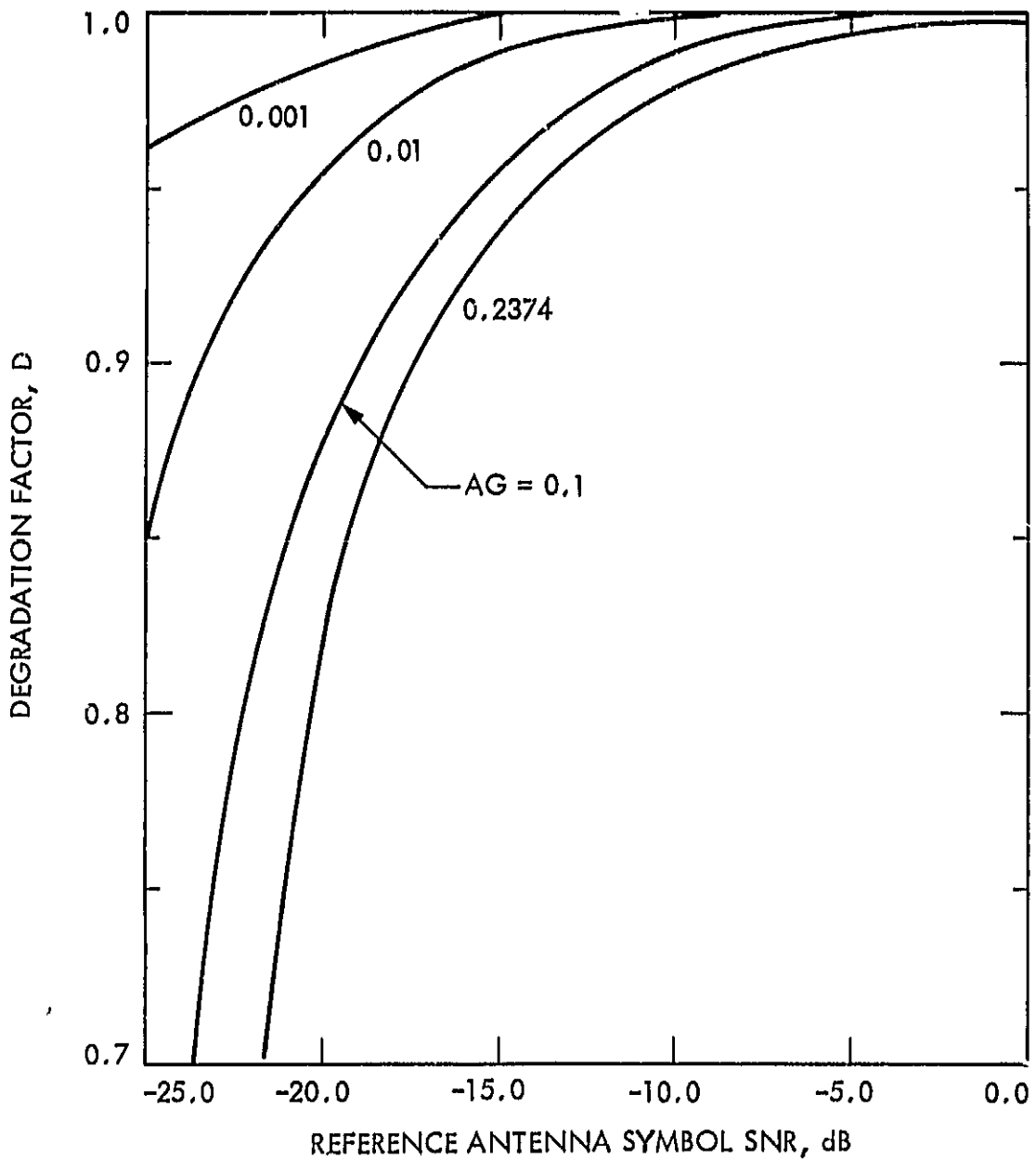


Figure 17. Degradation Factor vs. Symbol SNR, VRM Mission, $L = 4$. Other conditions include: noise bandwidth (B_n) = 3.75×10^6 Hz, symbol rate (r) = 550×10^3 sps, subcarrier frequency = 900×10^3 Hz, integration time = 1 second, $g = 0.3$, and $S_i = S_1/4$; $i = 2, \dots, L$.

1. Report No. 84-94, Rev. 1	2. Government Accession No.	3. Recipient's Catalog No.	
4. Title and Subtitle Performance Analysis of the DSN Baseband Assembly (BBA) Real-Time Combiner (RTC)		5. Report Date May 1, 1985	6. Performing Organization Code
7. Author(s) Marvin K. Simon and Alex Mileant		8. Performing Organization Report No.	
9. Performing Organization Name and Address JET PROPULSION LABORATORY California Institute of Technology 4800 Oak Grove Drive Pasadena, California 91109		10. Work Unit No.	11. Contract or Grant No. NAS7-918
12. Sponsoring Agency Name and Address NATIONAL AERONAUTICS AND SPACE ADMINISTRATION Washington, D.C. 20546		13. Type of Report and Period Covered External Report JPL Publication	
15. Supplementary Notes This revision corrects a computational error that was found after publication.		14. Sponsoring Agency Code RE211 BG-314-30-53-20-02	
16. Abstract The operation of the BBA Real-Time Combiner (RTC) is discussed and its performance investigated in detail. It is shown that each channel of the RTC can be modelled by a simple block diagram in the z-transform domain from which all pertinent transient and steady state behavioral characteristics can be determined. In particular, the characteristic equation of the tracking loop and its equivalent noise bandwidth are found and used to evaluate the closed loop transient response and steady-state mean squared timing jitter. The impact of the totality of these loop jitter contributions on the combiner output SNR is evaluated and illustrated numerically. These results show that for parameters of interest to various space missions, the RTC is capable of providing significant SNR improvement relative to a single receiving antenna.			
17. Key Words (Selected by Author(s)) Communications; Pioneer Project; Voyager Project		18. Distribution Statement Unclassified; unlimited	
19. Security Classif. (of this report) Unclassified	20. Security Classif. (of this page) Unclassified	21. No. of Pages	22. Price